Numerical methods to determine calcium release flux from calcium transients in muscle cells

J. Timmer*, T. Müller*, W. Melzer**

Keywords: muscle, calcium release, model fitting, smoothing

Running title: Numerical methods to estimate Ca^{2+} release

*Fakultät für Physik
Albert-Ludwigs-Universität
Hermann-Herder-Str. 3
D – 79104 Freiburg
**Abteilung für Angewandte Physiologie
Universität Ulm
Albert-Einstein-Allee 11
D – 89069 Ulm
Corresponding author: W.M.

ABSTRACT

Several methods are currently in use to estimate the rate of depolarization-induced calcium release in muscle cells from measured calcium transients. One approach first characterizes calcium removal of the cell. This is done by determining parameters of a reaction scheme from a fit to the decay of elevated calcium after the depolarizing stimulus. In a second step, the release rate during depolarization is estimated based on the fitted model. Using simulated calcium transients with known underlying release rates we tested the fidelity of this analysis in determining the time course of calcium release under different conditions. The analysis reproduced in a satisfactory way the characteristics of the input release rate even when the assumption that release had ended before the start of the fitting interval was severely violated. Equally good reconstructions of the release rate time course could be obtained when the model used for the analysis differed in structure from the one used for simulating the data. We tested the application of a new strategy (multiple shooting) for fitting parameters in non-linear differential equation systems. This procedure rendered the analysis less sensitive to ill chosen initial guesses of the parameters and to noise. A locally adaptive kernel estimator for calculating numerical derivatives allowed good reconstructions of the original release rate time course from noisy calcium transients when other methods failed.

INTRODUCTION

In muscle cells, force development is controlled by Ca^{2+} ions which are rapidly released from the sarcoplasmic reticulum during sarcolemmal depolarization (Ríos and Pizarro, 1991; Schneider, 1994; Melzer et al., 1995). The calcium concentration change resulting from this release can be measured using optical indicators while there is no direct way to measure the actual release flux. Various methods have been applied to derive the time course and magnitude of the Ca^{2+} release rate from the measured Ca^{2+} transient (Baylor et al., 1983; Melzer et al., 1984; Schneider et al., 1985; Melzer et al., 1987; Brum et al., 1988b; Sipido and Wier, 1991; García and Schneider, 1993; Gonzáles and Ríos, 1993; Pape et al., 1993; Delbono and Meissner, 1996; Shirokova et al., 1996). In these methods, it has to be taken into account that released Ca^{2+} flows to various myoplasmic compartments whose time-dependent Ca^{2+} contents have to be quantified.

Two principally different approaches for estimating calcium release have been described. Both start from kinetic models with binding and transport sites for Ca^{2+}. This leads to a system of non-linear differential equations. Only the compartment comprised by the indicator is observable. From the indicator signal the concentration of free calcium can be estimated. One approach uses tabulated kinetic parameters of the model and calculates all the occupancies by using the measured free calcium transient assuming that the literature values apply approximately to the experimental situation (Baylor et al., 1983; Sipido and Wier, 1991; Pape et al., 1993). The other approach tries to determine at least some of the kinetic parameters of the compartment model by analyzing the measured Ca^{2+} signals themselves (Melzer et al., 1984; Melzer et al., 1987; Brum et al., 1988b; García and Schneider, 1993; Gonzáles and Ríos, 1993; Delbono and Meissner, 1996; Shirokova et al., 1996). Thereby it is assumed that Ca^{2+} release which is induced by depolarization is completely and rapidly stopped after repolarization of the membrane. During the time after repolarization Ca^{2+} is redistributed among the model compartments. The relaxation time course of free calcium can be predicted with the model equations and compared with the actually measured time course. This comparison allows to optimize the parameters in such a way that the calculated relaxation deviates minimally from the measured one. The best fit parameters together with measured Ca^{2+} transients are then used to calculate the total release as the sum of all Ca^{2+} occupancies at each point of time. The rate of Ca^{2+} release is computed as the time derivative of this sum. Different varieties of this removal fit procedure have been used for analyzing Ca^{2+} measurements from skeletal muscle fibers (Melzer et al., 1986; Melzer et al., 1987; Brum et al., 1988a; Gonzáles and Ríos, 1993).

For routine application, this approach requires numerical algorithms which safely lead to a best fit even when the initial parameter guesses are far off from the best ones and which can handle a certain degree of noise in the experimental data, especially since derivatives have to be estimated by some smoothing procedure. For this purpose we tested several numerical methods which had been developed for other fields in recent years. For the tests, a simple Ca^{2+} compartment model and constructed Ca^{2+} release rate waveforms were used to simulate free calcium transients similar to those which can be measured in muscle fibers during voltage clamp depolarization (Melzer et al., 1987; Brum et al., 1988b; Feldmeyer et al., 1990). The numerical methods are judged by their ability to reliably determine the input model parameters and release rate time course. We show that the more refined strategies for fitting and smoothing improve the procedure for Ca^{2+} release calculation and we describe how noise and a violation of the model assumptions can affect the result. Finally, we show that simulation studies can help to decide if a simplified model is still able to yield reliable release rate estimates.

METHODS

Simulation

The model system of ordinary differential equations (ODE) chosen for this investigation is non-stiff and can be solved numerically by virtually any ODE integrator. For the computations presented here, the routines `ODEINT` and `BSSTEP` (Press et al., 1992) were used.

Normally distributed random numbers, generated by the routine `GASDEV` (Press et al., 1992), were added to the simulated transients to produce noisy synthetic data sets.

Parameter estimation

The parameters of the Ca^{2+} dynamics model were estimated from the simulated data using the method of least squares. The function $f(t, \mathbf{p})$ is the solution at time t of the observable part of the model ODE system with the parameter vector $\mathbf{p}$. Given measurements y_i with error variances σ_i^2 at times t_i, $1 \leq i \leq N$, the objective function

$$\chi^2(\mathbf{p}) = \sum_{i=1}^{N} \left(\frac{y_i - f(t_i, \mathbf{p})}{\sigma_i} \right)^2 \tag{1}$$

was minimized with respect to $\mathbf{p}$, giving a maximum likelihood estimate for $\mathbf{p}$.

Fitting parameters in a system of non-linear ODEs is cumbersome. As the model function $f(t, \mathbf{p})$ depends nonlinearly on the parameters, the fitting routine has to proceed iteratively, starting from some given initial guess for the parameters. In each iteration, an update step for the estimated parameters has to be computed which will decrease the discrepancy between the model and the given data. The update step is usually computed from the gradient (steepest descent method) or the Hesse matrix (Newton resp. Gauss-Newton method) of the objective function, or from a combination of both (Levenberg-Marquardt algorithm). The steepest descent method uses a linear approximation of the objective function, whereas the other methods use a quadratic approximation.

In contrast to non-linear parameter estimation in regression, in ODE systems, no analytical derivatives of the objective function can be supplied. The derivatives can be computed only numerically through finite differences,

$$\frac{\partial f(t_i, \mathbf{p})}{\partial p_j} \approx \frac{f(t_i, p_1, ..., p_j + h, ..., p_n) - f(t_i, \mathbf{p})}{h} \,. \tag{2}$$

The high computational effort of evaluating $f(t, \mathbf{p})$ usually does not allow for a higher order approximation. Therefore, the choice of h can be rather influential. Generally, h should be taken as some fractional part, 0.001 say, of p_j, with appropriate modifications if $p_j \approx 0$. The use of internal differentiation can reduce the computational effort substantially (Hairer et al., 1987).

It is well known that ill chosen initial estimates of the parameters can preclude most routines from yielding any solution at all because the trial trajectory diverges. In an interactive laboratory environment, this poses no principal problems as the routine can be started again with new initial parameters until convergence is reached. For routine data analysis, however, robust algorithms should be employed.

Since $\chi^2(\mathbf{p})$ shows a non-linear dependence on the parameters $\mathbf{p}$, $\chi^2(\mathbf{p})$ will usually have several local minima apart from the true global one that corresponds to the true parameters. Most parameter estimation routines signal convergence of their minimizing iteration if they can not reduce $\chi^2(\mathbf{p})$ in a small neighborhood of the actual parameter values any further. Thus, they might return estimates of $\mathbf{p}$ which are far from the desired true values. If the routine used does not include a strategy for circumventing this problem, every fit has to be inspected by eye in order to find out whether the desired global minimum has been reached.

Two methods for minimizing $\chi^2(\mathbf{p})$ are compared in this paper.

Initial value approach

If the problem of parameter identification in ODE systems is treated in the same way as other problems of non-linear regression, one is led to the so-called initial value approach: Starting from some initial values for the trial trajectory, the model equations are solved over the whole fitting interval and $\chi^2(\mathbf{p})$ is calculated. Derivatives are computed by finite differences. Then, the parameters are adjusted in such a way as to bring the solution closer to the data.

Quite often, the measurement at the beginning of the fitting interval is taken as a fixed initial value for the solution of the model equations, while estimates for the unobserved components are taken from a solution of the ODE system with given parameters along the measurement curve.

For computing the update step, several strategies have been proposed, e.g., the Gauss-Newton method (Schittkowski, 1995) or the Levenberg-Marquardt algorithm (Stortelder, 1996).

Multiple shooting

The technique of multiple shooting has been used for solving boundary value problems in ODE systems (Stoer and Bulirsch, 1993). In the context of parameter estimation, the method was introduced by van Domselaar and Hemker (1975) and, in a much more general context, by Bock (1981, 1983). The observation motivating the use of multiple shooting for parameter estimation is that with the initial value approach, one is effectively neglecting information on the dynamics of the system present in the measurements. Even though the time course of at least one component of the ODE system is known relatively accurately, the initial value approach does not take advantage of any but the very first observation in the fitting interval. If the initial parameters are far off from the correct ones, the trial trajectory can deviate arbitrarily far from the measurements.

With Bock's elegant approach, one partitions the fitting interval into many subintervals. The ODE system is solved separately on each of these intervals, using as starting guesses for the initial values the measurements at the beginning of these intervals. None of these initial values are fixed to the observations during the iteration. The initial values at these points have thus become new parameters of the model.

This approach leads to an initially discontinuous trajectory, which is, however, close to the measurements. The final trajectory must of course be continuous, i.e., the computed solution at the end of one subinterval must finally equal the initial value at the beginning of the next subinterval. In order to enforce this condition, continuity constraints are imposed on the solution. In each iteration, the method has to choose an update step which will not only lead to a minimum of the objective function $\chi^2(\mathbf{p})$, but which will also satisfy the continuity constraints in a linearized form. In this way, the newly introduced additional parameters, viz., the initial values at the mesh points, are eliminated from the linearized problem which has to be solved in order to compute the update step.

Since only the linearized continuity constraints are imposed on the update step, the iteration is allowed to proceed to the final continuous solution through "forbidden ground": the iterates will generally be discontinuous trajectories. This freedom allows the method to stay close to the observed data, prevents divergence of the numerical solution and reduces the problem of local minima.

As constraints on the parameters or trajectories (e.g., nonnegativity constraints on all rate constants and concentrations in the calcium model) are frequently helpful to further stabilize the fit, general constraints can be allowed for by taking their linearizations into account when computing the update step. To this end, a solver for linear systems with constraints has to be used (Stoer, 1971).

For the reduction of $\chi^2(\mathbf{p})$, a Gauss-Newton method is employed which effectively uses a second order approximation to $\chi^2(\mathbf{p})$ even though only first derivatives are involved. It can be further stabilized by an appropriate damping strategy which reduces the stepsize if the problem is highly non-linear. The rank-deficient case, e.g., when parameters or combinations of parameters cannot be identified reliably, can be treated elegantly by an appropriately chosen rank decision criterion.

Details of the mathematical and implementational aspects of the method are given in Bock (1981, 1983).

Data smoothing and the computation of derivatives of noisy data

In order to extract the release flux from given Ca^{2+} transients and model parameters, the intracellular Ca^{2+} dynamics has to be reconstructed from the data. This procedure involves integrating the ODE system along the noisy Ca^{2+} measurements and computing the derivative of the measurement curve.

In the present context, the data are interpreted as

$$y_i = f(t_i) + \epsilon_i, \tag{3}$$

where $f(t)$ is the model function and ϵ_i is the measurement error at time t_i, assumed to be normally distributed. When the parameters are known or have been estimated from the data, the smooth curve $f(t)$ underlying the measurements y_i can be identified.

Given data y_i, $1 \leq i \leq N$, sampled at a resolution of Δt, which are noisy observations of the underlying smooth curve $f(t)$, the derivative $f'(t_i)$ can be estimated by one-sided finite differences as

$$\hat{f}'(t_i) = \frac{y_{i+h} - y_i}{h\Delta t} \tag{4}$$

or by symmetric differences as

$$\hat{f}'(t_i) = \frac{y_{i+h} - y_{i-h}}{2h\Delta t}, \tag{5}$$

which is equivalent to exploiting the local Taylor series of $f(t)$ to first or second order, respectively. Generalizing this idea, one can try to fit polynomials of a fixed degree k to intervals of the observed data. If the intervals are such that the Taylor series to k-th order is a good approximation for $f(t)$, one can take the 0-th and first coefficient of the fitted polynomial as an estimate for $f(t)$ and its derivative, respectively. The choice of the correct interval width is essential for the reliability of this method.

With evenly spaced data, such as usually obtained by sampling, this technique can be realized efficiently as a weighted moving average. This method is known as the Savitzky-Golay smoothing filter (Savitzky and Golay, 1964; Press et al., 1992) or as Polynomial Least Squares Convolution (PLSC) (Ratzlaff, 1987). In the context of estimating Ca^{2+} release from Ca^{2+} transients, it has been proposed by Klein et al. (1988).

The Savitzky-Golay smoothing filter is in fact a special case of a more general class of methods known as kernel estimators. The basic idea of kernel estimation is to convolve the measurement with a so-called kernel function $K(\theta)$ in order to obtain estimates $\hat{f}(t_i)$ for the underlying function $f(t_i)$:

$$\hat{f}(t_i) = \sum_{j=-b}^{b} y(t_{i+j})\, K(j). \tag{6}$$

Kernel estimators can also be used to estimate derivatives. Kernel functions for derivatives have to satisfy certain moment conditions. By Gasser et al. (1985), a family of so-called optimal kernels was introduced which is known to have good analytical and practical properties. These kernels were used for the computations in the present paper.

As already noted for the Savitzky-Golay smoothing filter, the choice of the interval which is used to obtain an estimate for $f(t)$ is crucial for the performance of the method. In the context of kernel estimation, the width of this interval, equal to $2b + 1$ (cf. Eq. 6), is called the bandwidth.

If b is chosen too small, random variations in the data due to observational noise will be "interpreted" as belonging to the signal, thus yielding unsatisfactory results which tend to fluctuate around the true curve. This phenomenon is known as undersmoothing. If, on the other hand, b is chosen too large, the curve will be oversmoothed, resulting in the depression of peaks in the data and therefore in a bias of the estimate.

As peaks and even their amplitudes are extremely important in the physiological interpretation of the release rate, oversmoothing can hardly be tolerated. Undersmoothing, on the other hand, can amplify spurious effects in the data to such an extend that their amplitude is of the same size as that of the relevant physiological features.

There exist several techniques for choosing the bandwidth b adaptively from the given data (Müller and Stadtmüller, 1987; Seather, 1992). The resulting bandwidth will inevitably still lead to oversmoothing in some parts of the data, while other parts will be undersmoothed. One can therefore think of locally adapting b to the structure of the data, decreasing it at peaks and increasing it in flat sections.

Quantitatively, the locally optimal bandwidth of a kernel estimator for the ν-th derivative of $f(t)$ is inversely proportional to the square of the $(\nu + 2)$-th derivative of $f(t)$, e.g., of the third derivative of $f(t)$ if one wants to estimate $f'(t)$. In order to take these variations into account, one has to estimate the third derivative of the data. This can be done with an appropriate kernel estimator for which, due to the large variance of the estimate, a rather large bandwidth should be chosen. Mathematical as well as implementational details of this method are given by Müller (1988), which also contains further references to the literature. For the problem discussed here, a fixed bandwidth of 50 ms was chosen to estimate the third derivative.

Boundary effects were treated by generating pseudodata outside the measurement interval as described by Hall and Wehrly (1991), as the behavior of the measured curve long before and long after the depolarization is well known.

Statistics

Confidence intervals for the parameters were obtained from the Hesse matrix

$$H_{ij} = \frac{\partial^2 \chi^2(\mathbf{p})}{\partial p_i \, \partial p_j} \tag{7}$$

of the model equations at the best-fit parameters. It has to be assumed that the model is specified correctly and that the quadratic approximation of $\chi^2(\mathbf{p})$ holds in a large enough region around the solution point. Then, the matrix $C = (1/2\, H)^{-1}$ is the covariance matrix of the standard errors of the parameters, and the errors of the parameters are multivariately normally distributed with variances c_{ii} (Honerkamp, 1994). Independent 95% confidence intervals for p_i are given by $\hat{p}_i \pm 1.96 \cdot (c_{ii})^{1/2}$.

In some of the simulations presented below we use noiseless data. In these cases, instead of Eq. 1, we minimize the sum over the squared differences between the data and the model predictions. Consequently, no confidence intervals for the parameters can be given.

Hardware and software

The code written for this paper is part of an interdisciplinary project. Because of the different computer platforms involved, portability was a crucial issue. The programs were written in C/C++ and run on IBM RS/6000 workstations, PCs with the MS-DOS and PCs with the LINUX operating system.

Model simulations

For the simulation of artificial Ca^{2+} records we constructed rate of release waveforms which were used as input flux functions in a simplified Ca^{2+} distribution model.

The calcium release rate in skeletal muscle has been shown to reach a maximum value within a few milliseconds after the onset of a strong depolarization (Baylor et al., 1983; Melzer et al., 1984; Melzer et al., 1987; Simon and Schneider, 1988). It then falls to a considerably lower value probably resulting from a Ca^{2+}-dependent inactivation (Schneider and Simon, 1988; Simon et al., 1991; Jong et al., 1993; Jong et al., 1995; Chandler et al., 1995) and finally declines to zero with a very slow time course due to the combined action of SR depletion (Schneider et al., 1987) and voltage sensor inactivation (Brum et al., 1988b). Even though published release rates vary considerably, the fundamental characteristics, i.e., an early peak followed by a more or less steady level, seem to be conserved in different preparations (Melzer et al., 1987; García and Schneider, 1993; Delbono et al., 1995; Delbono and Meissner, 1996; Shirokova et al., 1996). We constructed release rate records which exhibited a fixed ratio of peak amplitude to steady level of 2:1 by using Eq. 8.

$$r(t) = \begin{cases} 0 & \text{for } t \leq 0, \\ s - ae^{-t/\tau_1} + (a-s)e^{-t/\tau_2} & \text{for } 0 < t \leq T, \\ -ae^{-t/\tau_1} + (a-s)e^{-t/\tau_2} + se^{-(t-T)/\tau_r} & \text{for } t > T. \end{cases} \tag{8}$$

Here τ_1 and τ_2 are the time constants for the rise and decline of the initial peak, respectively. The constant a defines an overall scaling of the curve, whereas s defines the steady level. The values used for our calculations are given in the legend of Fig. 1.

please locate Fig. 1 here

By varying the depolarization time T, release records of different duration were constructed (see Fig. 1A). The decline of the release after repolarization is determined by the time constant τ_r which was set to a low value of 3 ms in all simulations except the one described in connection with Figs. 9 and 10.

Fig. 1B shows the calcium distribution model that was used for the simulations. It is virtually identical with the one used by Melzer et al. (1986, 1987) to analyze Ca^{2+} removal and release in voltage-clamped frog muscle fibers, apart from the fact that the Ca^{2+} indicator is not included as a separate compartment in the present model. It was chosen to illustrate the use of the analysis algorithms because it has a small number of parameters and still exhibits the main characteristics of calcium distribution in muscle cells, i.e., fast and slow binding and slow uptake.

The model contains an instantaneously equilibrating non-saturating compartment CaF whose occupancy is a multiple (factor F) of the free calcium concentration (Eq. 9), a saturable slow compartment CaS, described by rate constants k_{on} and k_{off} and total concentration of binding sites S_{total} (Eq. 10), and a slow non-saturable uptake Ca_{up} with associated fixed rate constant k_{ns} (Eq. 11).

$$\dot{\text{CaF}} = F \cdot \dot{\text{Ca}}_{\text{free}} \tag{9}$$

$$\dot{\text{CaS}} = k_{\text{on}} \cdot \text{Ca}_{\text{free}} \cdot (\text{S}_{\text{total}} - \text{CaS}) - k_{\text{off}} \cdot \text{CaS} \tag{10}$$

$$\dot{\text{Ca}}_{\text{up}} = k_{\text{ns}} \cdot \text{Ca}_{\text{free}} \tag{11}$$

The time derivatives of the concentrations obey a conservation law:

$$\dot{\text{Ca}}_{\text{rel}}(t) = \dot{\text{Ca}}_{\text{free}}(t) + \dot{\text{CaF}}(t) + \dot{\text{CaS}}(t) + \dot{\text{Ca}}_{\text{up}}(t)\,, \tag{12}$$

where $\dot{\text{Ca}}_{\text{rel}}(t)$ is the rate of calcium release.

The parameters were chosen to be close to those determined by Melzer et al. (1986) to fit calcium transients measured in frog muscle fibers (see legend of Fig. 1). A peak amplitude of the input calcium release rate of $2\,\mu$M/ms was chosen to generate transients with characteristics similar to those measured in muscle cells (Fig. 1C). A series of five simulations obtained with release durations T of 20, 50, 100, 150 and 200 ms was used for the various analyses of this investigation. Fig. 1 shows the release rates (A) and the occupancies of the calcium compartments Ca_{free} (C), Ca_{up} (D), and CaS; the latter one at two different time scales (E, F).

For the chosen range of release rates the slow saturable compartment reached saturation levels between 21 and 91%. This leads to a progressive slowing of the relaxation phases in the five free calcium records with increasing release duration. The saturation of this slow compartment reduces its participation in the removal of Ca^{2+} from compartments Ca_{free} and CaF. It is necessary to include in the analysis records with low and with large saturation of CaS if one wants to precisely identify the parameters k_{on}, k_{off} and S_{total}.

Determining the release rate

The first step in determining release from given Ca^{2+} transients is a characterization of Ca^{2+} removal. For this purpose, a Ca^{2+} distribution model is used to fit the relaxation phases of measured Ca^{2+} transients. The fit returns a set of kinetic model parameters to describe removal. The only a priori assumption on release is that it is turned off after repolarization. Therefore, it is assumed that the relaxation phases of the free calcium transients reflect redistribution of calcium in and removal from the myoplasmic space involving fluxes between compartments $\mathrm{Ca_{free}}$, CaF, CaS and $\mathrm{Ca_{up}}$. In general, the model used will at best be a good approximation to the real situation in the cell. In the present case, however, the model structure used for analyzing the simulated calcium transients is identical with the model used for simulation. Therefore, we expect that the values of the four free parameters k_{on}, k_{off}, $\mathrm{S_{total}}$, and k_{ns} can precisely be determined from the information contained in the different calcium relaxation phases (F was set to the true value of 30).

please locate Fig. 2 here

Fig. 2 shows that this is indeed the case. Stages 1 and 2 of the figure show start and end of the iterative process in which a 150 ms interval of each relaxation phase of the five simulated calcium records was fitted with the numerical solution of Eqs. 9 to 11 with respect to $\mathrm{Ca_{free}}$. Starting values for the fit were as follows: $k_{\mathrm{on}} = 5\,\mu\mathrm{M}^{-1}\mathrm{s}^{-1}$, $k_{\mathrm{off}} = 0.15\,\mathrm{s}^{-1}$, $\mathrm{S_{total}} = 50\,\mu\mathrm{M}$, $k_{\mathrm{ns}} = 200\,\mathrm{s}^{-1}$.

The fitting procedure works in two steps. First, the given calcium transients and initial suggestions for the parameters are used to calculate the occupancies of the non-observable Ca^{2+} compartments (CaF, CaS and $\mathrm{Ca_{up}}$). At 15 ms after the start of the release turn-off, the mode of calculation is changed. Now Eqs. 9 to 11 are used to calculate free calcium using the values at the end of the first calculation as initial values for the integration. Since the parameter values are different from the true ones, the calculated curves (bold lines) deviate from the simulated calcium records (Fig. 2, stage 1). A least squares minimization algorithm which searches for a minimum of the objective function $\chi^2(\mathbf{p})$ modifies the parameters until the Euclidean norm of the update step is less than some fractional amount, e.g. 10^{-3}, of the norm of the parameter vector. We do not use relative change of $\chi^2(\mathbf{p})$ as a criterion because numerical experience shows that this may lead to premature signaling of convergence in some cases (Gill et al., 1981).

In the example shown in Fig. 2 it took three iterations for the fitting algorithm to converge (stage 2). As noted in the figure legend, the parameters found by the fit approximated the true parameters with deviations of less than 1%. Convergence to the absolute minimum of the objective function depends on the choice of the parameter starting values. If these starting values are too far off from the true values the algorithms might proceed to a local minimum comprising considerably worse fits or might even diverge. A substantial improvement can be obtained by using the so-called multiple shooting approach introduced by Bock (1981).

Based on the best fit parameters, the occupancies of all compartments are calculated. Their sum yields the released calcium (Fig. 2, stage 3). Finally, the rate of release is given by the derivative of the released calcium (Fig. 2, stage 4).

RESULTS

In this section we first compare the initial value and the multiple shooting approach for parameter estimation in differential equations. Then we investigate the different smoothing algorithms to estimate derivatives of noisy data. Finally we examine how violations of the model assumptions influence the estimated rate of release.

Comparison of two fit algorithms

We first compare the two algorithms with respect to their convergence behavior if the starting guesses for the parameters are varied.

please locate Fig. 3 here

Application of the multiple shooting procedure is exemplified in Fig. 3. For this figure, the starting values were chosen to be substantially off the true parameter values: $k_{\text{on}} = 1\,\mu\text{M}^{-1}\text{s}^{-1}$, $k_{\text{off}} = 1\,\text{s}^{-1}$, $\text{S}_{\text{total}} = 1\,\mu\text{M}$, $k_{\text{ns}} = 1\,\text{s}^{-1}$.

Given these starting guesses for the parameters, the initial value approach (left) was unable to return estimates for the parameters, as the trajectory of one of the unobserved compartments in the model diverged during the iteration. The multiple shooting algorithm (right), however, succeeded after eleven iterations (Fig. 3F) and estimated the parameter values with equal precision as in the case of Fig. 2.

please locate Tab. 1 here

As expected, this algorithm proved its superiority when the deviation of the starting values from the true parameter values was large. Table 1 summarizes the results of a number of runs with the two algorithms in which different sets of starting values were tried. Furthermore, we compared the performance of the algorithms with respect to positivity constraints on the parameters and investigated the effect of fixing the first point of the trial trajectory to the observation. The entries denote the numbers of iterations until convergence. In several cases, the procedure stopped because the trial trajectories diverged (D). In one instance, no convergence was obtained within 100 iterations (N). Twice, a local minimum in parameter space was reached (L). When no constraints were imposed on the parameters, both routines failed to converge in a large number of cases. Also, fixing the first fitting point (FIX) to the observation proved to be destabilizing. Thus, positivity constraints and a freely varying first point (FREE) should be included in any strategy. As can be seen from the fifth column of Tab. 1, the multiple shooting approach was able to handle much larger deviations of the starting values from the true parameters than the initial value approach. In the one case where the multiple shooting algorithm failed, the introduction of small positive (instead of zero) lower bounds on the parameters led to convergence, whereas the initial value approach still diverged.

please locate Fig. 4 here

please locate Fig. 5 here

The multiple shooting algorithm proved to be especially helpful when noisy records were analyzed. Here the fact that also the initial values of the fitting intervals are optimized was of considerable advantage. The five artificial Ca^{2+} records of Fig. 1 were subjected to noise by adding normally distributed random numbers with standard deviations σ ranging from 0.005 to $0.2\,\mu$M while the largest amplitude reached in the calcium transients was $1.5\,\mu$M. Fig. 4 shows examples with four different noise levels. Fits were carried out with each set of records. An example is shown in Fig. 5. It demonstrates the result of the removal fit with three selected records from the total number of five calcium transient ($\sigma = 0.2\,\mu$M). The true records (dashed lines) and fitted trajectories (bold lines) are superimposed on the noisy records.

Fig. 5A shows the effect of fixing the first point of the fitted trajectory to the observation at the beginning of the fitting interval. As this value deviates far from the underlying true curve, the final trajectory could not reproduce the data adequately. In the example shown, the release rates computed with the parameters obtained from this fit were unsatisfactory. If the initial value was allowed to vary freely (Fig. 5B), the fit reproduced the data adequately, and the true parameters could be identified within the predicted error margins.

please locate Tab. 2 here

Table 2 summarizes the result of fits to the same original records but subjected to different levels of noise and compares the results for the two algorithms considered. In each case, three different variants were investigated (for details, see table legend). The multiple shooting algorithm was superior over the conventional initial value approach in that it produced convergence more reliably at larger noise levels.

Smoothing algorithms and numerical derivatives

The second stage in the rate of release recalculation involves the following step: The model equations, now supplied with the best fit values of the free parameters, are used to calculate the Ca^{2+} occupancies of CaF, Ca_{up} and CaS by using as input function a given calcium transient (i.e., the observed function representing Ca_{free}). All four compartment concentrations are summed (Fig. 2, stage 3). Assuming that no Ca^{2+} was present initially, this yields the estimated time course of the total calcium released. To derive the rate of release, a function reflecting the gating of the release channels, the summed total calcium has to be differentiated numerically (Fig. 2, stage 4). This can easily be done by using a difference approximation (Eq. 5, METHODS) if the records are smooth. However, as soon as noise is involved the numerical derivative poses severe problems. To a certain degree this can be overcome by means of signal averaging. Yet, since not all preparations allow for time-consuming signal averaging, one has to look for optimal procedures to carry out the analysis with noisy records. In the following, we compare the quality of three different ways of estimating numerical derivatives and describe the errors in the calculated rate of release introduced by each one. The first procedure is the conventional difference approximation (Eq. 5). The second method (kernel estimation with globally chosen bandwidth) smoothes the noisy record by a weighted moving average, which is equivalent to fitting polynomials locally. This has the advantage that the derivative can be calculated analytically from the fitted parameters. The choice of the interval length over which each local fit is carried out results from an analysis of the noise variance σ^2.

A more refined method (local adaptive algorithm, see Müller, 1988) adjusts the interval length by estimating the local curvature of the signal by means of a crude estimate of the third derivative of the record. This reduces oversmoothing at locations where the signal changes steeply and uses larger smoothing intervals in regions where the curvature is small.

please locate Fig. 6 here

The details of the procedure are demonstrated in Fig. 6. Here, the numerical derivative of a simulated free calcium transient with Gaussian noise ($\sigma = 0.1\,\mu$M, comp. Fig. 4C) is calculated. The original record (with and without noise) is shown in Fig. 6A. Panel B shows the estimated third derivative used in the kernel estimator, calculated with a fixed bandwidth of 50 ms (see METHODS) and panel C the resulting kernel bandwidth for each point in time chosen by the algorithm. The continuous line in panel D shows the first time derivative of the noisy calcium transient determined with the locally varying kernel bandwidth of panel C. For comparison, the dashed line shows the true derivative of the noise-free transient. The positive peak at the beginning of the time course is underestimated by 23 %. This difference results from the trade-off between bias and variance of the estimator. Choosing a smaller bandwidth in this region would decrease the bias but increase the variance. The chosen bandwidth minimizes the expected mean-square error which combines bias and variance.

please locate Fig. 7 here

Fig. 7 compares a number of methods for calculating the numerical derivative in the determination of the rate of calcium release. Three different noise levels in the simulated calcium records were applied (see legend). In order to exclude effects due to different realizations of the noise, we used identical realizations scaled to different amplitudes (panel A). In each case, the true values of the model parameter were used for the calculation of the compartment occupancies in order to exclude variability due to different quality of the removal model fit. Fig. 7B shows the application of the locally adaptive approach outlined in Fig. 6. It produces a rather smooth record and yet gives a relatively good reconstruction of the rapid components of the original rate of release curve (dashed line) even for the highest level of noise. From left to right, the calculated peak amplitudes were 98, 83, and 86% of the original one. In contrast, a kernel estimator with optimal global bandwidth (panel C) considerably underestimated the initial peak rate for the larger levels of noise (99, 67, 66%). Lowering the global bandwidth in an attempt to get better peak restoration also considerably increased the noise (Fig. 7D). This was even more the case when a difference approximations of the numerical derivative was used. A choice of the bandwidth ($h = 4$) that gave good peak restoration completely failed at the higher noise levels (panel F) and increasing the bandwidth to lower the noise ($h = 10$) strongly suppressed the peak (panel G).

please locate Fig. 8 here

Fig. 8 demonstrates the outcome of the complete analysis procedure in the presence of noise. It compares the standard analysis used in the original description of the procedure (Melzer et al., 1987), i.e., initial value method for parameter estimation by removal fit and finite differences for derivatives on one hand (left column), with the multiple shooting method combined with the adaptive kernel estimator on the other hand (right column). Apart from the major problems regarding the numerical derivatives, the standard procedure introduced further deviations in the release calculation due to the unreliability in estimating the model parameters and failed to calculate a tolerable estimate of the rate of release time course. The new methods, however, led to a result that stayed close to the original record even under these unfavorable conditions.

In summary, while for relatively clean records (left column of Fig. 7) even a difference approximation with small bandwidth (Fig. 7F) gives good results, the only method that could cope with the higher noise levels was the locally adaptive kernel estimator (Fig. 7B).

The latter method offers a more reliable estimation of the release rate. This holds for the reconstruction of the peak at the beginning of the depolarization as well as for the flat parts of the release rate time course.

Violation of the model assumptions

A crucial assumption for the removal model fit analysis is that release can be turned off rapidly by repolarization. Only this enables an independent characterization of removal by inspecting the decay of free calcium. If release is still present during the decay, one can expect that removal will be underestimated and the calculated release time course during the depolarization will be in error. To assess this possible error we increased the turn-off time constant τ_r of the input calcium release signals (Eq. 8) and analyzed the resulting free calcium transients in the same way as before. Fig. 9 shows the result of this analysis for four different turn-off time constants. While the peak of the release rate was not affected, increasing τ_r produced an increasingly stronger slowly decaying undershoot below the actual plateau level. Therefore, delayed closure of the release channels would cause an apparent increase in the ratio of peak to steady level of the determined rate of release.

please locate Fig. 9 here

Fig. 10 explains this result. The figure compares the contribution of the different calcium compartments to the total release rates derived with the removal model fit in two different cases. On the left, a rapid ($\tau_r = 3\,\mathrm{ms}$) and on the right a slow ($\tau_r = 25\,\mathrm{ms}$) turn-off of the release had been used for the calcium transient simulation. For the slowly ceasing release, 55% of the steady state level of release was still active at the time the fit started.

please locate Fig. 10 here

As the model used for fitting assumes that release has turned off completely 15 ms after repolarization, this condition is forced upon the estimated release rate, thereby distorting its shape. Especially the slow saturable component is too small (Fig. 10, right panel).

Inspecting the best fit parameter values (Fig. 10 legend) shows that this is mainly due to a significant underestimation of S_{total} (43 vs. 101 μM). An additional underestimation of the non-saturable removal parameter k_{ns} (330 vs. 400 s^{-1}) contributes only little to the underestimation of the removal rate (Fig. 10D, right panel).

Effects of misspecified removal models on the estimated release

In the preceding paragraphs we investigated how the quality of the release rate estimate obtained from the removal model fit approach depends on factors like the level of noise in the data, the numerical procedure used for calculating derivatives and the degree to which the assumption that release stops immediately after repolarization is fulfilled.

To ensure that the model used for the fit could reproduce the characteristics of Ca^{2+}

removal in the system underlying the calculated free calcium data, we used exactly the same model for generating the data. When analyzing measured data, however, the model used for the fit will at best be an approximation to the real system. In general, the models will be misspecified. This misspecification might show up in different ways :

1. The model does not contain as many compartments as the real system.

2. Some parameters of the model are fixed to values that are not equal to the true ones.

3. The kinetic scheme of the model does not correspond to the real system.

There is no straightforward way to decide if the model used for the fit can sufficiently reproduce the main characteristics of Ca^{2+} release in the experimental system. The criterion generally used to decide if a given model suffices for the analysis is the quality of the removal fit. A model which does not lead to a good fit of the relaxation time course can be assumed to be insufficient for the release calculation. On the other hand, it is assumed, even though not unambiguously proven, that a model which leads to a good fit of the Ca^{2+} relaxation time course after repolarization under different conditions will correctly describe the overall removal properties of the cell and will, therefore, lead to a good approximation of the release rate time course. We believe that this criterion needs further evaluation in future investigations.

It seems more straightforward to decide if a given removal model (which fits the real data well) can be replaced by a simpler model. Here too, the simulation approach offers a valuable tool. Free calcium data resembling real ones can be simulated using a detailed model and can then be analyzed using models comprising less parameters or even a different kinetic structure. If release rates obtained from the analysis are close to the known ones used for the simulation it seems to be justified to substitute the simpler model for the more complex one. In applications this may offer the possibility to use a model in which all parameters are identifiable from the given data.

We demonstrate this approach with two examples shown in Fig. 11. As before, we used the release rates of Fig. 2A and generated free calcium transients with the model displayed in Fig. 2B.

For the model used in the removal fit analysis we used a different structure. The rate constant k_{ns} was changed to a function that decreased with the amount of released calcium. For this purpose the fractional saturation f of the site S was calculated (Eq. 13, obtained from Eq. 10 after dividing by $\mathrm{S_{total}}$) and was assumed to modify the uptake rate according to Eq. 14, which replaces Eq. 11.

$$\dot{f} = k_{\mathrm{on}} \cdot \mathrm{Ca_{free}} \cdot (1-f) - k_{\mathrm{off}} \cdot f \tag{13}$$

$$\dot{\mathrm{Ca}}_{\mathrm{up}} = (a-f) k_{\mathrm{ns}}^{0} \cdot \mathrm{Ca_{free}} \tag{14}$$

I. e. $a\, k_{\mathrm{ns}}^{0}$ is the effective uptake rate constant at zero saturation of S whereas $(a-1)\, k_{\mathrm{ns}}^{0}$ is the value at full saturation.

The new model reproduced the slowing of relaxation of the calcium transients which in the original scheme resulted from the progressive filling of the slow buffer S. In the new scheme, S was eliminated as a buffer by assuming that $\mathrm{S_{total}}$ had a negligibly small value. Thus, calcium bound to the slow system S does not influence the calcium distribution directly. The uptake in the new scheme can be envisaged to become partially inactivated by a calcium-dependent mechanism that contributes a negligible amount of calcium binding sites. For a further simplification we set the parameter k_{off} to zero. Thus, the resulting model (model I) contained one parameter less than the model used for generating the data.

Fig. 11A displays the calcium transients and the removal fits. Fig. 11B compares the synthetic release rates (dashed lines) and those calculated based on the simpler model (solid lines). Apart from a slight underestimation of the plateau the time courses are in good agreement. Fig. 11C shows the removal fits for the case that the parameter a in Eq. 14 is fixed to 1 (model II) which means that uptake is completely suppressed when S is fully saturated. The quality of the fit is only slightly worse than that in Fig. 11A, but the estimated release rates in Fig. 11D differ qualitatively from the original ones in showing an increase instead of a steady level and negative going phases at the end of the shorter depolarizations.

DISCUSSION

The determination of the Ca^{2+} release rate from the sarcoplasmic reticulum has been used frequently to characterize excitation-contraction coupling in muscle cells (Baylor et al., 1983; Melzer et al., 1984; Schneider et al., 1985; Melzer et al., 1987; Brum et al., 1988b; Sipido and Wier, 1991; Jacquemond and Schneider, 1992; García and Schneider, 1993; Gonzáles and Ríos, 1993; Pape et al., 1993; Delbono, 1995; Delbono et al., 1995; Pape et al., 1995; Delbono and Meissner, 1996; Shirokova et al., 1996; Jong et al., 1996). An empirical determination requires several steps of analysis including the fit of a removal model to experimental calcium transients (Melzer et al., 1986; Melzer et al., 1987; Brum et al., 1988a; Gonzáles and Ríos, 1993; Shirokova et al., 1996).

In the present work we examined under defined conditions to which degree the analysis gives correct results. For this purpose, we applied known release rate waveforms to a known, completely identifiable calcium turnover model so that the result of the analysis could easily be compared with the true data and the influence of various disturbing factors on the analysis result could be studied. We described several mathematical tools which can help to improve the method.

The main questions studied were the following: 1. How can the non-linear removal fit be optimized? 2. To which degree can the release determination cope with observational noise in the calcium records? 3. How sensitive are the results to a violation of the main assumption of the removal fit analysis, namely, that release is completely turned off after repolarization? 4. Is it possible to use simplified removal models comprising fewer parameters?

There is no general procedure that prevents divergence of the removal model fit or convergence into a local minimum of the parameter space. Compared with the classical initial value approach, the multiple shooting algorithm which divides the fit interval into smaller subintervals showed clear advantages. It reduces the inherent numerical instability of the initial value approach which results from its high sensitivity to the initial choice of the parameter values. The multiple shooting procedure requires less effort for searching for a suitable set of initial parameter guesses because it converges to the correct values for a larger range of initial guesses than the initial value approach. It seems particularly useful when noisy records are to be analyzed. By including the measured concentration values at several points of time during the free calcium decay as initial values for a discontinuous initial trajectory, the multiple shooting fit uses the available dynamic information of the system more efficiently. The reformulation of the initial value problem into a multipoint boundary value problem forces the trajectory to stay close to the measured data and therefore reduces the chance of divergence even for ill chosen starting values. Since the actual linearized problem which has to be solved has the same dimension as the initial value problem the multiple shooting algorithm does not require significantly more calculation time. We think that this method will be of advantage in applications where short lifetimes of the preparation (e.g. patch clamp experiments on isolated myocytes or neurons) prohibit time consuming signal averaging.

The physics underlying the Ca^{2+} compartment model imposes certain constraints on the parameters. Most notably, rate constants and concentrations must be non-negative. Numerical experience shows that fitting algorithms tend to diverge if these constraints are violated. Therefore, it seems natural to implement them as part of the fitting procedure. Our simulation studies showed that positivity constraints on the parameters do indeed stabilize the fitting procedure substantially.

In the presence of noise, convergence to a local minimum was not a serious problem with the multiple shooting approach whereas this could easily occur in the initial value approach. With regard to the latter one additional point should be noted. It has been common practise in previous work with the removal fit method to fix the first point of the fitted trajectory to the observation at the beginning of the fitting interval. However, there is no real justification for this procedure. Instead, the initial value should be treated as an additional free parameter to be fitted. Indeed our simulations showed that fixing the first point destabilized the procedure both in the absence and even more in the presence of noise.

Noise is even more a problem when numerical derivatives have to be calculated. This is required in all available methods of determining the release rate, be it deductive (Baylor et al., 1983) or inductive (Melzer et al., 1987; Brum et al., 1988b). Furthermore, it is necessary when kinetic limitations of indicator dyes have to be corrected for (Klein et al., 1988). There are definitely limits for off-line analysis to correct for noise and experiments should be designed to reduce it as much as possible beforehand. Among the algorithms we compared, the kernel estimator with locally adaptive optimization of the filter bandwidth showed the best results in preserving fast changes and flat sections of the release rate. Difference approximations of the time derivative should only be used when the records have a high signal-to-noise ratio.

The quality of the estimated release rate time course depends not only on the numerical methods applied, but also on the validity of the central assumption that there is no residual release during the decay phase of the calcium signal which is used for the removal model fit.

We investigated the effect of a violation of this assumption by allowing increasing overlap between the analysis interval and slowly decaying release. The calculated release rate underestimated the true one and was temporally distorted. This showed up in an increased ratio of peak to steady level and in a shallow minimum of the release rate right after the peak (Fig. 9D). From an analysis of the temporal behavior of the model compartments, this effect could be explained with an underestimation of the slow saturable removal component. Overall, however, the main temporal characteristics were rather well preserved even in cases where the overlap was large.

Larger models including more details of the calcium turnover kinetics than the one used here have been applied for semi-empirically deriving the rate of release in muscle fibers (Brum et al., 1988b; Gonzáles and Ríos, 1993). In these models, not all the kinetic parameters can be simultaneously identified and therefore only a subset of parameters can be obtained by the fit while others have to be fixed beforehand. Moreover, models realistically describing the intracellular situation during Ca release will also have to include diffusion of both Ca and some of its target site populations and will have to appreciate the fact that the myoplasm is not uniform in terms of Ca release (Ríos and Stern, 1997). Ca is released from distinct regions within the sarcomer, which can create substantial local concentration gradients.

For the purpose of this paper, i.e. for demonstrating the advantages of improved numerical methods, we chose the present relatively unsophisticated calcium distribution model, simply because of the small number of model parameters involved. However, the general conclusions regarding the benefits of the multiple shooting algorithm combined with an adaptive kernel estimator for deriving the rate of release also hold for more complicated reaction schemes introduced in previous publications.

The problem of actually selecting a minimal kinetic scheme for the removal model fit appropriate for given experimental results was not the scope of this study. However, with the example of Fig. 11 we demonstrate that the approach of analyzing artificial free calcium transients simulated with known release rates may be applied for the purpose of model reduction, i.e. to decide if a given model can be substituted by a simpler one. A simpler model can be trusted to fulfill its task equally well if it reliably returns the known release rates used for the simulation. Conclusions exclusively based on the apparent fit quality, however, may be misleading. The result of Fig. 11C and D indicates that a satisfactory fit does not necessarily guarantee perfect reconstruction of the underlying release rate waveform. We therefore feel that one should be cautious in overinterpreting small kinetic details of the release rates determined from muscle cells and that the general issue of optimal model selection requires further mathematical investigation.

In summary, we showed that advanced methods of data analysis for fitting ODEs as well as for estimating derivatives from noisy data allow for a more reliable reconstruction of the release rate time course than the commonly applied methods. Since the methods investigated here showed their full power in the presence of noise, they will be particularly useful when the time-resolved transmembrane calcium flux is to be determined from calcium transients of smaller cells (cultured myocytes, neurons etc.) which produce signals with lower signal-to-noise ratios than skeletal muscle fibers.

Acknowledgments: We would like to thank W. Horbelt for valuable discussions, Drs J.

Honerkamp and F. Lehmann-Horn for their support, B. Dietze and A. Struk for technical help and Dr M. Schiebe for initiating the cooperation. This work was supported by a grant of the Deutsche Forschungsgemeinschaft to W.M.

References

Baylor, S. M., Chandler, W. K., and Marshall, M. W. 1983. Sarcoplasmic reticulum calcium release in frog skeletal muscle fibres estimated from arsenazo III calcium transients. *J. Physiol.*, 334:625–666.

Bock, H. G. 1981. Numerical treatment of inverse problems in chemical reaction kinetics. *In* Modelling of Chemical Reaction Systems. Ebert, K., Deuflhard, P., and Jäger, W., editors. Springer, Heidelberg and New York. 102–125.

Bock, H. G. 1983. Recent advances in parameteridentification techniques for o.d.e. *In* Numerical Treatment of Inverse Problems in Differential and Integral Equations. Deuflhard, P. and Hairer, E., editors. Birkhäuser, Basel. 95–121.

Brum, G., Ríos, E., and Schneider, M. F. 1988a. A quantitative model of calcium removal from the myoplasmic solution (appendix to Brum et al. 1988b). *J. Physiol.*, 398:467–473.

Brum, G., Ríos, E., and Stéfani, E. 1988b. Effects of extracellular calcium on calcium movements of excitation-contraction coupling in frog skeletal muscle fibres. *J. Physiol.*, 398:441–473.

Chandler, W. K., Jong, D., Pape, P. C., and Baylor, S. M. 1995. Calcium inactivation of calcium release in frog skeletal muscle fibers. *In* Calcium as Cell Signal. Maruyama, K., Nonomura, Y., and Kohama, K., editors. Igaku-Shoin Medical Publishers, Inc., New York. 80–88.

Delbono, O. 1995. Ca^{2+} modulation of sarcoplasmic reticulum Ca^{2+} release in rat skeletal muscle fibers. *J. Membr. Biol.*, 146:91–99.

Delbono, O. and Meissner, G. 1996. Sarcoplasmic reticulum Ca^{2+} release in slow- and fast-twitch muscle. *J. Membr. Biol.*, 151:123–130.

Delbono, O., O'Rourke, K. S., and Ettinger, W. H. 1995. Excitation-calcium release uncoupling in aged single human skeletal muscle fibers. *J. Membr. Biol.*, 148:211–222.

Feldmeyer, D., Melzer, W., and Pohl, B. 1990. Effects of gallopamil on calcium release and intramembrane charge movements in frog skeletal muscle fibres. *J. Physiol.*, 421:343–362.

García, J. and Schneider, M. F. 1993. Calcium transients and calcium release in rat fast-twitch skeletal muscle fibres. *J. Physiol.*, 463:709–728.

Gasser, T., Müller, H.-G., and Mammitzsch, V. 1985. Kernels for nonparametric curve estimation. *J. R. Stat. Soc. B*, 47:238–252.

Gill, P. E., Murray, W., and Wright, M. H. 1981. Practical Optimization. Academic Press, London.

Gonzáles, A. and Ríos, E. 1993. Perchlorate enhances transmission in skeletal muscle excitation-contraction coupling. *J. Gen. Physiol.*, 102:373–421.

Hairer, E., Nørsett, S. P., and Wanner, G. 1987. Solving Ordinary Differential Equations I. Springer, Heidelberg and New York.

Hall, P. and Wehrly, T. E. 1991. A geometrical method for removing edge effects from kernel-type nonparametric regression estimates. *J. Am. Stat. Ass.*, 86:665–672.

Honerkamp, J. 1994. Stochastic Dynamical Systems. VCH, Weinheim.

Jacquemond, V. and Schneider, M. F. 1992. Effects of low myoplasmic Mg^{2+} on calcium binding by parvalbumin and calcium uptake by the sarcoplasmic reticulum in frog skeletal muscle. *J. Gen. Physiol.*, 100:115–135.

Jong, D.-S., Pape, P. C., Baylor, S. M., and Chandler, W. K. 1995. Calcium inactivation of calcium release in frog cut muscle fibres that contain millimolar EGTA or Fura-2. *J. Gen. Physiol.*, 106:337–338.

Jong, D.-S., Pape, P. C., Chandler, W. K., and Baylor, S. M. 1993. Reduction of calcium inactivation of sarcoplasmic reticulum calcium release by fura-2 in voltage-clamped cut twitch fibres from frog muscle. *J. Gen. Physiol.*, 102:333–370.

Jong, D.-S., Pape, P. C., Geibel, J., and Chandler, W. K. 1996. Sarcoplasmic reticulum calcium release in frog cut muscle fibers in the presence of a large concentration of EGTA. *In* Organellar Ion Channels and Transporters. Clapham, D. E., editor. The Rockefeller University Press, New York. 255–268.

Klein, M. G., Simon, B. J., Szücs, G., and Schneider, M. F. 1988. Simultaneous recording of calcium transients in skeletal muscle using high- and low-affinity calcium indicators. *Biophys. J.*, 53:971–988.

Melzer, W., Herrmann-Frank, A., and Lüttgau, H. C. 1995. The role of Ca^{2+} ions in excitation-contraction coupling of skeletal muscle fibres. *Biochim. Biophys. Acta*, 1241:59–116.

Melzer, W., Ríos, E., and Schneider, M. F. 1984. Time course of calcium release and removal in skeletal muscle fibers. *Biophys. J.*, 45:637–641.

Melzer, W., Ríos, E., and Schneider, M. F. 1986. The removal of myoplasmic free calcium following calcium release in frog skeletal muscle. *J. Physiol.*, 372:261–292.

Melzer, W., Ríos, E., and Schneider, M. F. 1987. A general procedure for determining the rate of calcium release from the sarcoplasmic reticulum in skeletal muscle fibers. *Biophys. J.*, 51:849–863.

Müller, H.-G. 1988. Nonparametric Regression Analysis of Longitudinal Data. Springer, Heidelberg and New York.

Müller, H.-G. and Stadtmüller, U. 1987. Variable bandwidth kernel estimators of regression curves. *Ann. Stat.*, 15:182–201.

Pape, P. C., Jong, D.-S., and Chandler, W. K. 1993. Effect of Fura-2 on action potential-stimulated calcium release in cut twitch fibers from frog muscle. *J. Gen. Physiol.*, 102:295–332.

Pape, P. C., Jong, D.-S., and Chandler, W. K. 1995. Calcium release and its voltage dependence in frog cut muscle fibers equilibrated with 20 mM EGTA. *J. Gen. Physiol.*, 106:259–336.

Press, W. H., Teukolsky, S. A., Vetter, W. T., and Flannery, B. P. 1992. *Numerical Recipes in C.* Cambridge University Press, Cambridge. Second edition.

Ratzlaff, K. L. 1987. Introduction to Computer-assisted Experimentation. Wiley, New York.

Ríos, E. and Pizarro, G. 1991. Voltage sensor of excitation-contraction coupling in skeletal muscle. *Physiol. Rev.*, 71:849–907.

Ríos, E. and Stern, M. D. 1997. Calcium in close quarters: Microdomain feedback in excitation-contraction coupling and other cell biological phenomena. *Annu. Rev. Biophys. Biomol. Struct.*, 26:47–82.

Savitzky, A. and Golay, M. J. E. 1964. Curve smoothing by local polynomial fits. *Analytical Chemistry*, 36:1627–1639.

Schittkowski, K. 1995. Parameter estimation in differential equations. *In* Recent Trends in Optimization Theory and Applications. Agarwal, R., editor. World Scientific, Singapore. 353–370.

Schneider, M. F. 1994. Control of calcium in functioning skeletal muscle fibers. *Annu. Rev. Physiol.*, 56:463–484.

Schneider, M. F., Ríos, E., and Melzer, W. 1985. Use of a metallochromic indicator to study intracellular calcium movements in skeletal muscle. *Cell Calcium*, 6:109–118.

Schneider, M. F. and Simon, B. J. 1988. Inactivation of calcium release from the sarcoplasmic reticulum in frog skeletal muscle. *J. Physiol.*, 405:727–745.

Schneider, M. F., Simon, B. J., and Szücs, G. 1987. Depletion of calcium from the sarcoplasmic reticulum during calcium release in frog skeletal muscle. *J. Physiol.*, 392:167–192.

Seather, S. J. 1992. The performance of six popular bandwidth selection methods on some real data sets. *Comp. Stat.*, 7:225–250.

Shirokova, N., García, J., Pizarro, G., and Ríos, E. 1996. Ca^{2+} release from the sarcoplasmic reticulum compared in amphibian and mammalian skeletal muscle. *J. Gen. Physiol.*, 107:1–18.

Simon, B. J., Klein, M. G., and Schneider, M. F. 1991. Calcium dependence of inactivation of calcium release from the sarcoplasmic reticulum in skeletal muscle fibers. *J. Gen. Physiol.*, 97:437–471.

Simon, B. J. and Schneider, M. F. 1988. Time course of activation of calcium release from sarcoplasmic reticulum in skeletal muscle. *Biophys. J.*, 54:1159–1163.

Sipido, K. R. and Wier, W. 1991. Flux of Ca^{2+} across the sarcoplasmic reticulum of guinea-pig cardiac cells during excitation-contraction coupling. *J. Physiol.*, 435:605–630.

Stoer, J. 1971. On the numerical solution of constrained least-squares problems. *SIAM J. Num. Anal.*, 8:382–411.

Stoer, J. and Bulirsch, R. 1993. Introduction to Numerical Analysis. Springer, Heidelberg and New York. Second edition.

Stortelder, W. J. H. 1996. Parameter estimation in chemical engineering, a case study for resin production. *In* Scientific Computing in Chemical Engineering. Keil, F., Mackens, W., Voß, H., and Werther, J., editors. Springer, Heidelberg and New York. 226–238.

van Domselaar, B. and Hemker, P. W. 1975. Nonlinear parameter estimation in initial value problems. Technical Report Report NW 18/75, Mathematical Centre Amsterdam.

Figure captions

Fig. 1 Construction of synthetic calcium transients.

(A) Ca^{2+} release rates calculated with Eq. 8. Parameters: $a = 4.6$, $s = 1$, $\tau_1 = 2\,\mathrm{ms}$, $\tau_2 = 5\,\mathrm{ms}$. Amplitude $2\,\mu\mathrm{M/ms}$. Off time constant, $\tau_r = 3\,\mathrm{ms}$. T had values of 20, 50, 100, 150 and 200 ms to simulate different durations of depolarization.

(B) Ca^{2+} distribution model used for the calculations in this paper.

(C) Synthetic free calcium transients simulated with the model (B), Eqs. 9–12 and synthetic release rates (A). Model parameters were as follows: Slow sites: $k_{\mathrm{on}} = 10\,\mu\mathrm{M}^{-1}\mathrm{s}^{-1}$; $k_{\mathrm{off}} = 0.3\,\mathrm{s}^{-1}$; $\mathrm{S}_{\mathrm{total}} = 100\,\mu\mathrm{M}$. Uptake: $k_{\mathrm{ns}} = 400\,\mathrm{s}^{-1}$. Expansion due to intrinsic fast sites, $F = 30$.

(D) Reuptake of Ca^{2+} into the SR.

(E) Occupancy of slow sites.

(F) Occupancy of slow sites on a larger time scale.

Fig. 2 Removal fit and release calculation.

Initial parameters were $k_{\mathrm{on}} = 5\,\mu\mathrm{M}^{-1}\mathrm{s}^{-1}$, $k_{\mathrm{off}} = 0.15\,\mathrm{s}^{-1}$, $\mathrm{S}_{\mathrm{total}} = 50\,\mu\mathrm{M}$, $k_{\mathrm{ns}} = 200\,\mathrm{s}^{-1}$. All five transients were fitted simultaneously.

(1) Thin lines: synthetic transients. Bold lines: initial trajectories produced by the fitting routine.

(2) Thin lines: synthetic transients. Bold lines: trajectories of the fitting routine upon convergence. Best-fit parameters : $k_{\mathrm{on}} = 9.95\,\mu\mathrm{M}^{-1}\mathrm{s}^{-1}$, $k_{\mathrm{off}} = 0.297\,\mathrm{s}^{-1}$, $\mathrm{S}_{\mathrm{total}} = 100.6\,\mu\mathrm{M}$, $k_{\mathrm{ns}} = 399.7\,\mathrm{s}^{-1}$. True parameters used for simulation: $k_{\mathrm{on}} = 10\,\mu\mathrm{M}^{-1}\mathrm{s}^{-1}$, $k_{\mathrm{off}} = 0.3\,\mathrm{s}^{-1}$, $\mathrm{S}_{\mathrm{total}} = 100\,\mu\mathrm{M}$, $k_{\mathrm{ns}} = 400\,\mathrm{s}^{-1}$.

(3) Occupancy of the model compartments, computed from the transients of (1) using best-fit parameters (shown for the longest depolarization only). (A) $\mathrm{Ca}_{\mathrm{free}} + \mathrm{CaF}$, (B) CaS, (C) $\mathrm{Ca}_{\mathrm{up}}$, (D) $\mathrm{Ca}_{\mathrm{rel}}$, equal to the sum of (A), (B) and (C).

(4) Release rates computed as the numerical derivative of Ca_{rel} (3D).

Fig. 3 Comparison of initial value approach and multiple shooting approach.

Fit of the synthetic transients of Fig. 1, using the ill chosen initial parameters $k_{on} = 1\,\mu M^{-1}s^{-1}$, $k_{off} = 1\,s^{-1}$, $S_{total} = 1\,\mu M$, $k_{ns} = 1\,s^{-1}$. All five transients were fitted simultaneously. Thin lines: synthetic transients. Bold lines: trajectory produced by the fitting routine.

Left: Initial value approach. The figure shows iterations 1 (A), 2 (C), and 3 (E). After the third iteration, the program stopped due to the divergence of one of the trajectories of the unobserved compartments.

Right: Multiple shooting approach with five subintervals. The figure shows iterations 1 (B), 3 (D), and 11 (F). The program signaled convergence after the eleventh iteration. Note that the trajectory is discontinuous during iterations 1 and 3.

Fig. 4 Synthetic Ca^{2+} transients with different noise levels.

Differently scaled identical realizations of normally distributed random numbers were added to the smooth transients shown in Fig. 1C. (A) $\sigma = 0.01\,\mu M$. (B) $\sigma = 0.05\,\mu M$. (C) $\sigma = 0.1\,\mu M$. (D) $\sigma = 0.2\,\mu M$.

Fig. 5 Removal fit of noisy synthetic calcium transients.

All five records of Fig. 4D ($\sigma = 0.2\,\mu M$) were fitted simultaneously; only three records are shown. Thin lines, simulated noisy transient. Dashed lines: underlying noise-free transient. Bold lines: best-fit trajectory.

(A) The initial value of the ODE system was fixed to the measurement at the beginning of the fitting interval. Best-fit parameters ($\pm$ standard errors): $k_{on} = 5 \pm 6\,\mu M^{-1}s^{-1}$, $k_{off} = 0 \pm 0.004\,s^{-1}$, $S_{total} = 266 \pm 447\,\mu M$, $k_{ns} = 0 \pm 761\,s^{-1}$.

(B) The initial value of the ODE system was allowed to vary freely. Best-fit parameters: $k_{on} = 13 \pm 4\,\mu M^{-1}s^{-1}$, $k_{off} = 0.04 \pm 0.18\,s^{-1}$, $S_{total} = 144 \pm 32\,\mu M$, $k_{ns} = 350 \pm 77\,s^{-1}$.

Fig. 6 Computation of the numerical derivative of a noisy free Ca^{2+} transient by locally adaptive kernel estimation.

(A) Synthetic noisy Ca^{2+} transient ($\sigma = 0.1\,\mu$M, cf. Fig. 4C).

(B) Estimate of third derivative (in μM/ms^3).

(C) Locally chosen kernel bandwidth (solid line). The globally optimal bandwidth (dashed line) is 36 ms.

(D) First derivative of the transient shown in (A). Solid line: derivative computed by locally adaptive kernel estimator (in μM/ms). Dashed line: analytical derivative of the noise-free transient.

Fig. 7 Comparison of numerical derivative procedures for the calculation of the rate of calcium release from calcium transients subjected to different levels of noise. The true values of the model parameters were used in each case; therefore, the variability results exclusively from the different ways of calculating the derivatives.

(A) Noisy synthetic transients, from left to right: $\sigma = 0.005$, 0.05 and 0.1 μM.

(B–G) Original (dashed line) and recalculated (continuous line) rate of release using the following methods of carrying out numerical derivatives of summed total calcium concentration (see Fig. 2):

(B) Local adaptive kernel estimator.

(C) Kernel estimator with optimal global bandwidth (left: 8 ms, middle: 27 ms, right: 36 ms).

(D) Kernel estimator with fixed bandwidth of 10 ms.

(E) Kernel estimator with fixed bandwidth of 50 ms.

(F) Finite differences, $h = 4$ (see Eq. 5).

(G) Finite differences, $h = 10$.

Fig. 8 Comparison of two analysis procedures for determining the rate of Ca^{2+} release from the noisy set of free calcium data of Fig. 4C ($\sigma = 0.1\,\mu$M).

Left: Canonically applied method. Right: Improved methods.

(A) Result of removal fit with the initial value approach with no constraints on the parameters and with the first point at the beginning of the fitting interval fixed to the observation. Best fit parameters: $k_{\mathrm{on}} = 3.4 \pm 2.0\,\mu\mathrm{M}^{-1}\mathrm{s}^{-1}$, $k_{\mathrm{off}} = -0.01 \pm 0.06\,\mathrm{s}^{-1}$, $\mathrm{S}_{\mathrm{total}} = 342 \pm 289\,\mu$M, $k_{\mathrm{ns}} = -83 \pm 381\,\mathrm{s}^{-1}$.

(B) Release rate computed by symmetrical finite differences, $h = 10$ (Eq. 5).

(C) Final trajectory of the multiple shooting approach (five subintervals) with positivity constraints on the parameters and with the first point at the beginning of each fitting interval as an additional free parameter. Best fit parameters: $k_{\mathrm{on}} = 11 \pm 2\,\mu\mathrm{M}^{-1}\mathrm{s}^{-1}$, $k_{\mathrm{off}} = 0.14 \pm 0.11\,\mathrm{s}^{-1}$, $\mathrm{S}_{\mathrm{total}} = 118 \pm 17\,\mu$M, $k_{\mathrm{ns}} = 376 \pm 43\,\mathrm{s}^{-1}$.

(D) Release rate computed by the locally adaptive kernel estimator.

Fig. 9 Consequences of delayed turn-off of release for the analysis result.

Free calcium transients were simulated with release rates with different τ_r (cf. Eq. 8). These transients were then fitted with the removal model, assuming that the release had turned off completely 15 ms after repolarization. Solid lines, release rates computed from the transients using best-fit parameters. Dashed lines, original release rates. The fractions of release still present at 15 ms after repolarization, in percent of the steady level ($1\,\mu$M/ms), were as follows (τ_r in parentheses): (A) 3% (3 ms). (B) 12% (7 ms). (C) 37% (15 ms). (D) 55% (25 ms).

Fig. 10 Result of release rate calculation for Ca^{2+} transients simulated with fast and slow turn-off of release.

Five calcium transients were generated from synthetic release rates with different τ_r (cf. Eq. 8). These transients were then fitted with the removal model, and release rates were computed with the resulting best-fit parameters. F was fixed to 30 in each case.

Left: $\tau_r = 3\,\mathrm{ms}$, i.e., fast release turn-off. Best fit parameters: $k_{\mathrm{on}} = 9.95\,\mu\mathrm{M}^{-1}\mathrm{s}^{-1}$; $k_{\mathrm{off}} = 0.29\,\mathrm{s}^{-1}$; $\mathrm{S}_{\mathrm{total}} = 100.6\,\mu\mathrm{M}$. $k_{\mathrm{ns}} = 399.7\,\mathrm{s}^{-1}$.

Right: $\tau_r = 25\,\mathrm{ms}$, i.e., slow release turn-off. Best fit parameters: $k_{\mathrm{on}} = 10.4\,\mu\mathrm{M}^{-1}\mathrm{s}^{-1}$; $k_{\mathrm{off}} = 0\,\mathrm{s}^{-1}$; $\mathrm{S}_{\mathrm{total}} = 43.4\,\mu\mathrm{M}$. $k_{\mathrm{ns}} = 330\,\mathrm{s}^{-1}$.

(A) Simulated transients (thin lines) and trajectory from the removal fit (bold lines).

(B) Total release rates.

(C) Rates of change for total fast calcium, i.e., $\dot{\mathrm{Ca}}_{\mathrm{free}} + \dot{\mathrm{Ca}}\mathrm{F}$.

(D) Rates of Ca^{2+} uptake, $\dot{\mathrm{Ca}}_{\mathrm{up}}$.

(E) Rates of change for slow calcium, $\dot{\mathrm{Ca}}\mathrm{S}$.

In B–E: Solid lines: computed. Dashed lines: original.

Fig. 11 Effects of misspecified removal models on the estimated release

(A) Synthetic free calcium transients (Fig. 1C) and removal fit of the misspecified model I (bold lines). Best fit parameters : $k^0_{\mathrm{ns}} = 944.5$, $k_{\mathrm{on}} = 10.88$, $a = 1.40$.

(B) True release rate (dashed lines) (Fig. 1A) and estimation based on the misspecified model I (solid lines).

(C) Synthetic free calcium transients (Fig. 1C) and removal fit of the misspecified model II (bold lines). Best fit parameters : $k^0_{\mathrm{ns}} = 990.5$, $k_{\mathrm{on}} = 3.21$.

(D) True release rate (dashed lines) (Fig. 1A) and estimation based on the misspecified model II (solid lines).

Table captions

Tab. 1 heading Comparison of initial value (IV) and multiple shooting (MS) approaches for different starting guesses of the parameters.

Tab. 1 caption True values: $k_{\mathrm{on}} = 10\,\mu\mathrm{M}^{-1}\mathrm{s}^{-1}$, $k_{\mathrm{off}} = 0.3\,\mathrm{s}^{-1}$, $\mathrm{S}_{\mathrm{total}} = 100\,\mu\mathrm{M}$, $k_{\mathrm{ns}} = 400\,\mathrm{s}^{-1}$. The parameter F was fixed to 30. MS3 and MS5 denote multiple shooting with 3 and 5 subintervals, respectively. The table gives the number of iterations needed for convergence. L: convergence to a local minimum in parameter space; D: divergent behavior; N: no convergence within 100 iterations. Results are shown for either no constraints or positivity constraints on the parameters. Furthermore, the first fitting point was either fixed (FIX) or treated as an additional free parameter (FREE).

Tab. 2 heading Convergence behavior of initial value (IV) and multiple shooting (MS) approach at six different noise levels σ.

Tab. 2 caption Two different sets of parameter starting values were chosen for the iteration (A, B). True model parameters: $k_{\mathrm{on}} = 10\,\mu\mathrm{M}^{-1}\mathrm{s}^{-1}$, $k_{\mathrm{off}} = 0.3\,\mathrm{s}^{-1}$, $\mathrm{S}_{\mathrm{total}} = 100\,\mu\mathrm{M}$, $k_{\mathrm{ns}} = 400\,\mathrm{s}^{-1}$, F fixed to 30. Starting values for the four free parameters are given in the same sequence with the same units.

IVa: no constraints on the parameters, first point fixed to observed value; IVb: as IVa but first point as additional free parameter; IVc: as IVb but with positivity constraints on all parameters.

MS3, MS5, and MS9 denote multiple shooting with positivity constraints on all parameters and with 3, 5, and 9 subintervals, respectively.

The table gives the number of iterations needed for convergence. L: convergence to a local minimum in parameter space; D: divergent behavior; N: no convergence within 100 iterations.

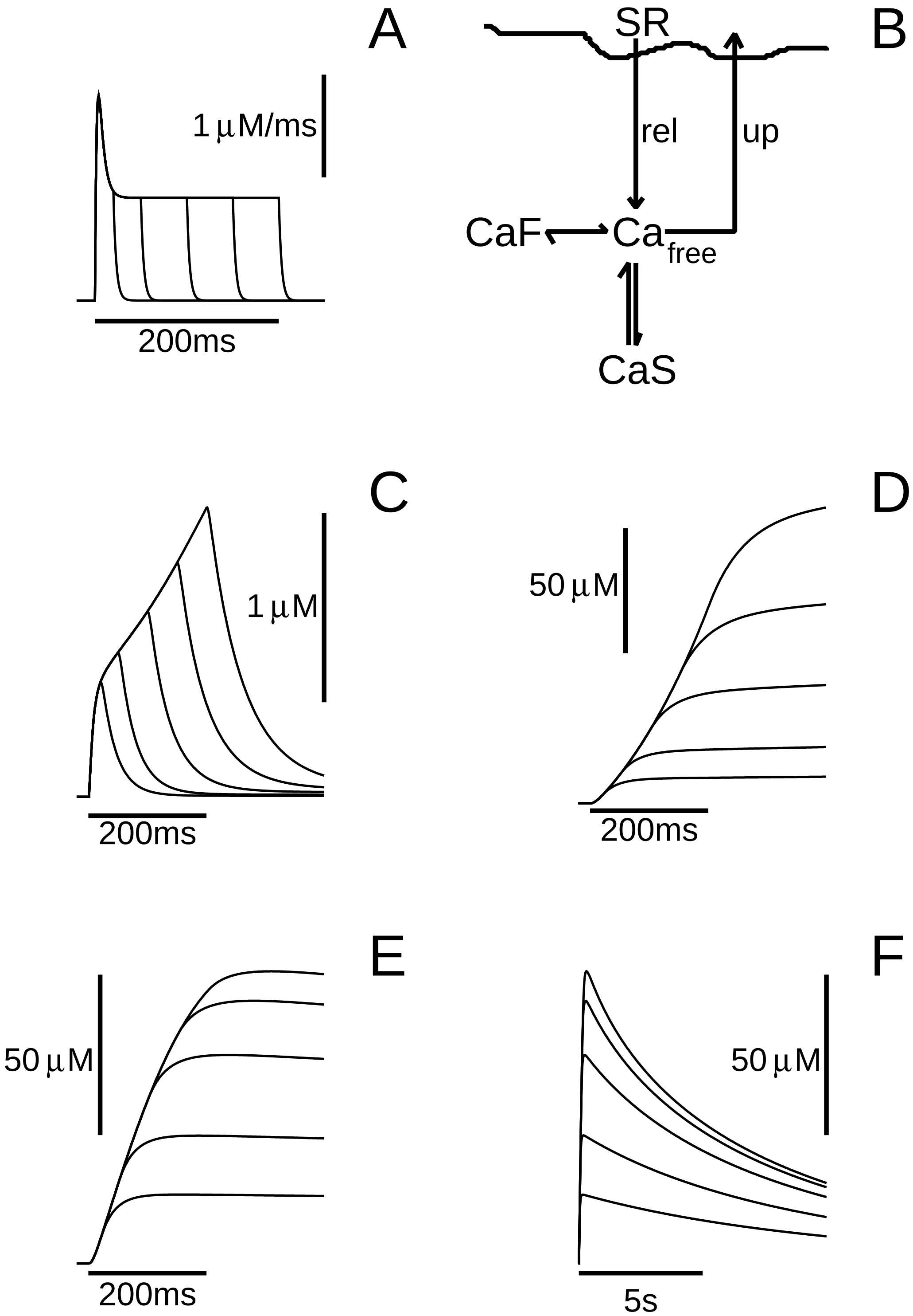
A
1 µM/ms
200ms
B
SR
rel
up
CaF
Ca_{free}
CaS
C
1 µM
200ms
D
50 µM
200ms
E
50 µM
200ms
F
50 µM
5s

Figure 1:

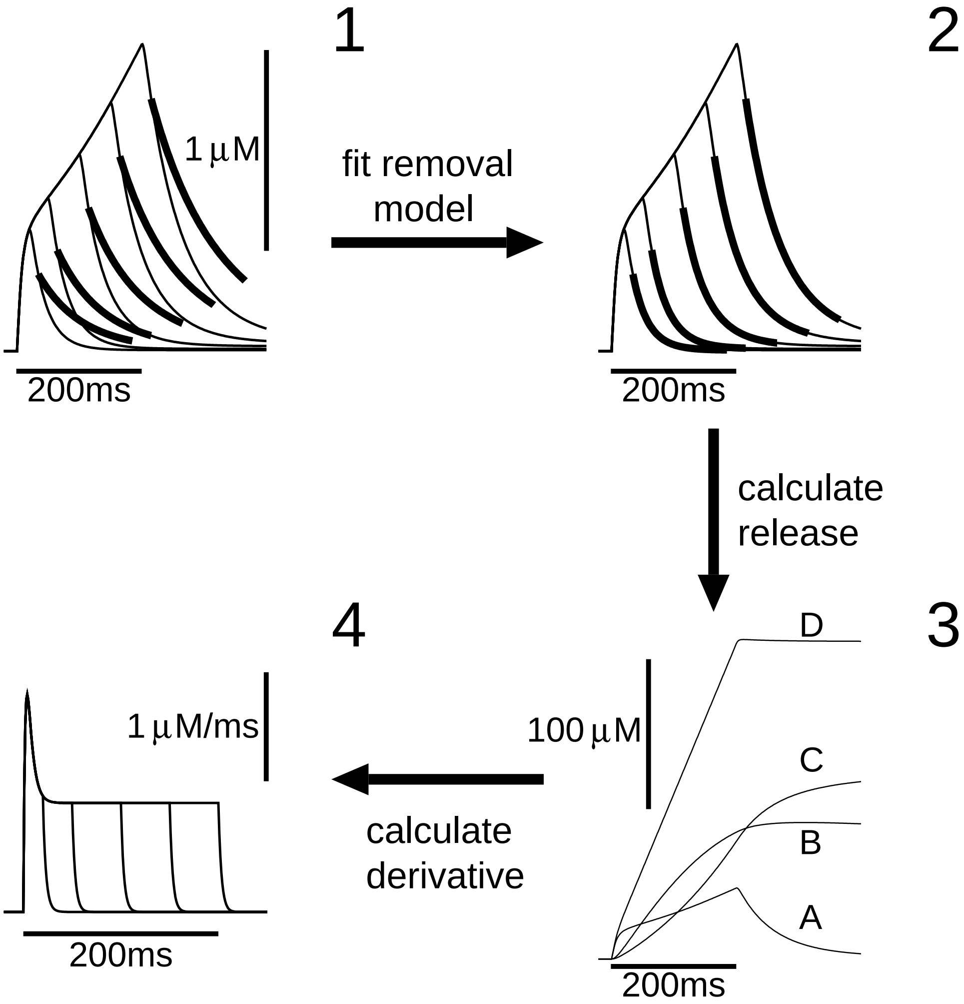
1
1 μM
200ms
fit removal
model
2
200ms
calculate
release
3
D
C
B
A
100 μM
200ms
calculate
derivative
4
1 μM/ms
200ms

Figure 2:

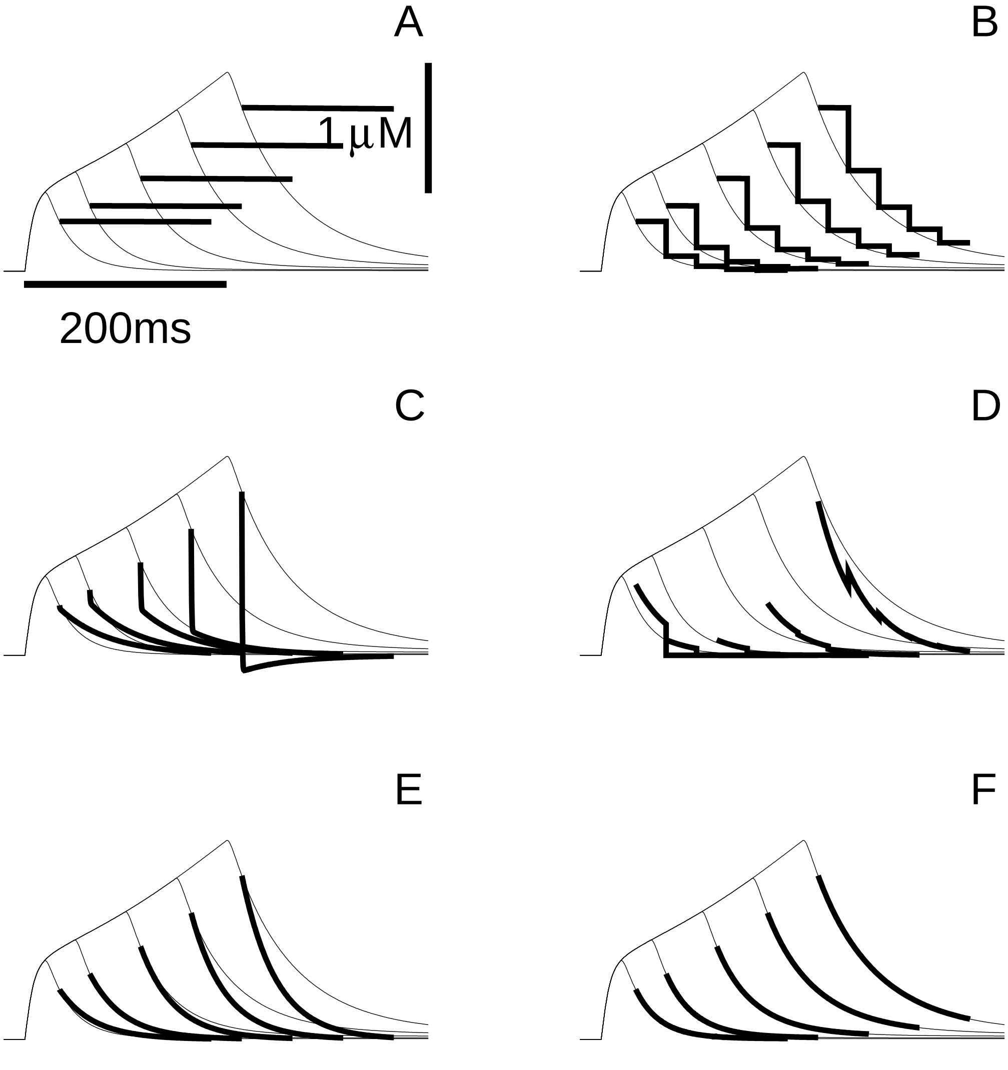

Figure 3:

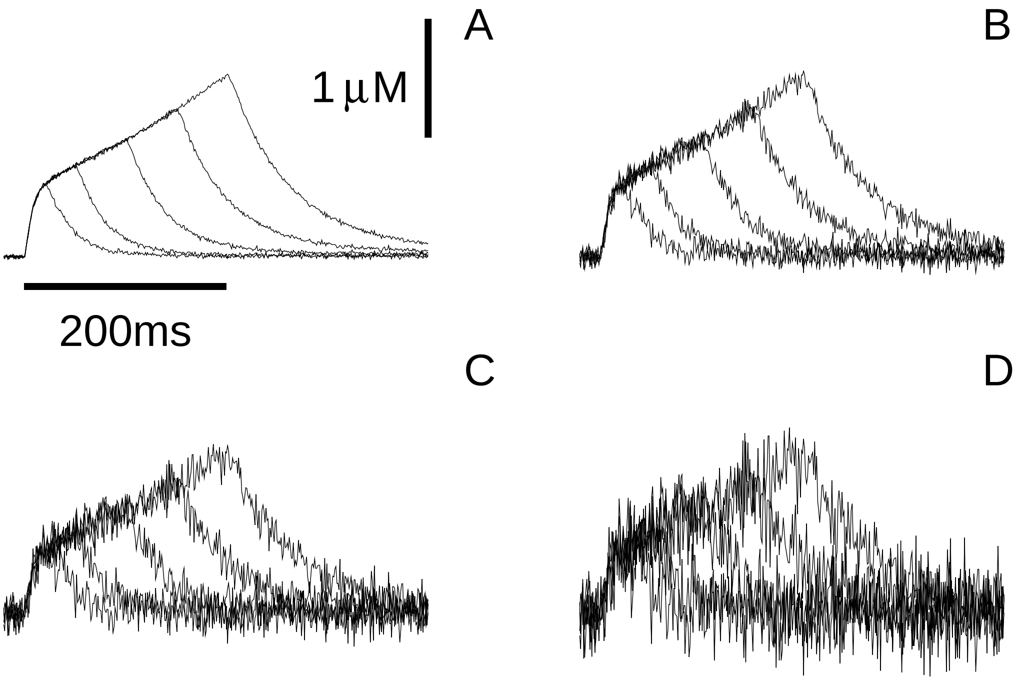

Figure 4:

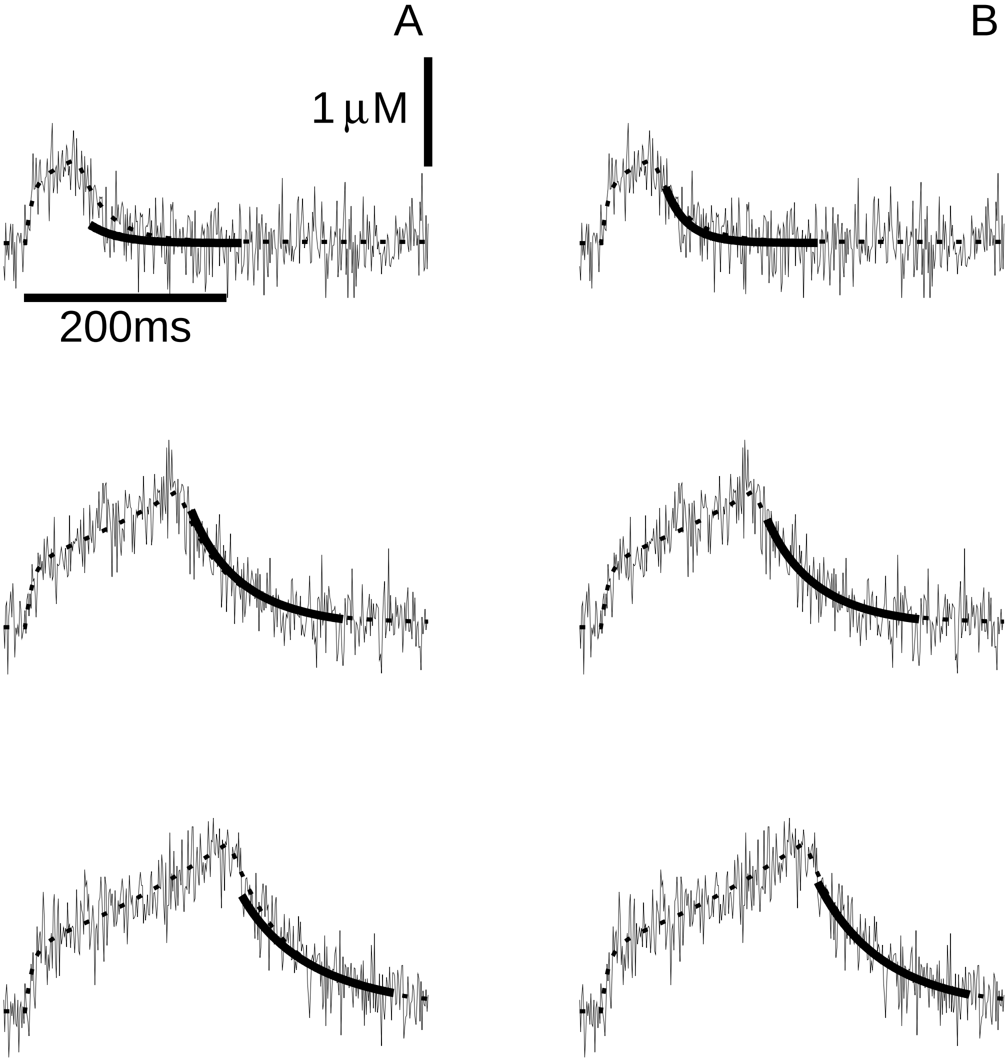

Figure 5:

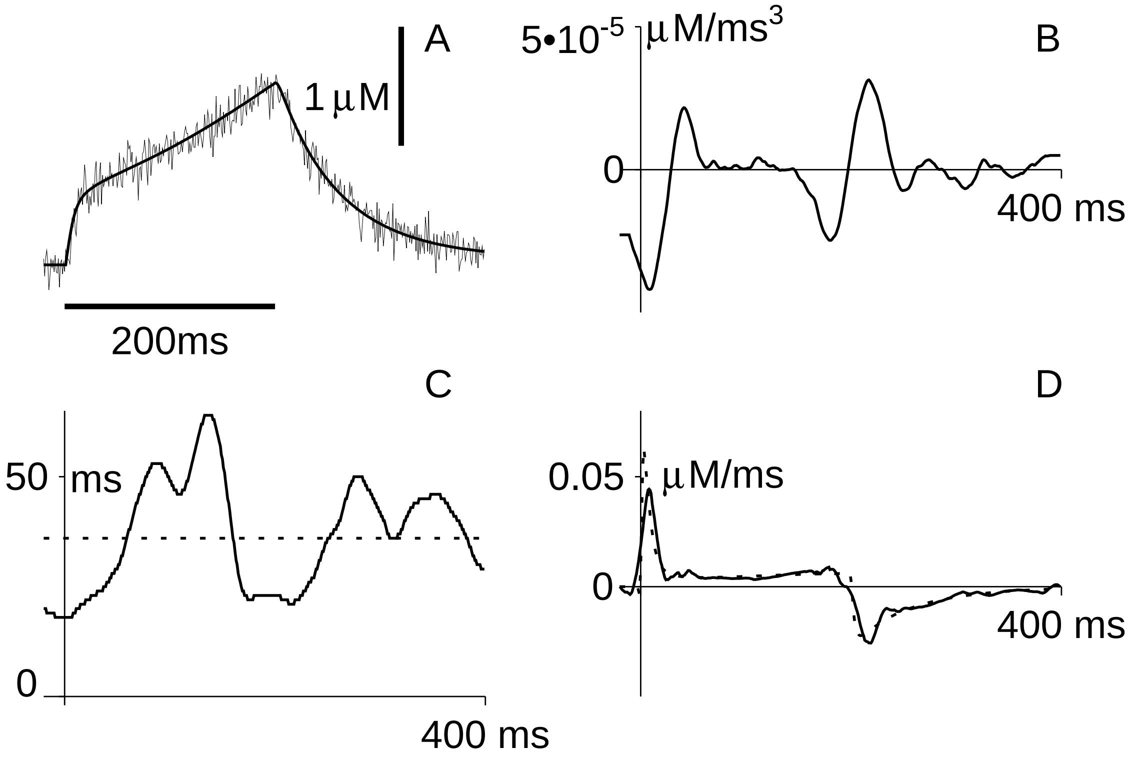

A
1 μM
200ms
B
5•10-5 μM/ms3
0
400 ms
C
50 ms
0
400 ms
D
0.05 μM/ms
0
400 ms

Figure 6:

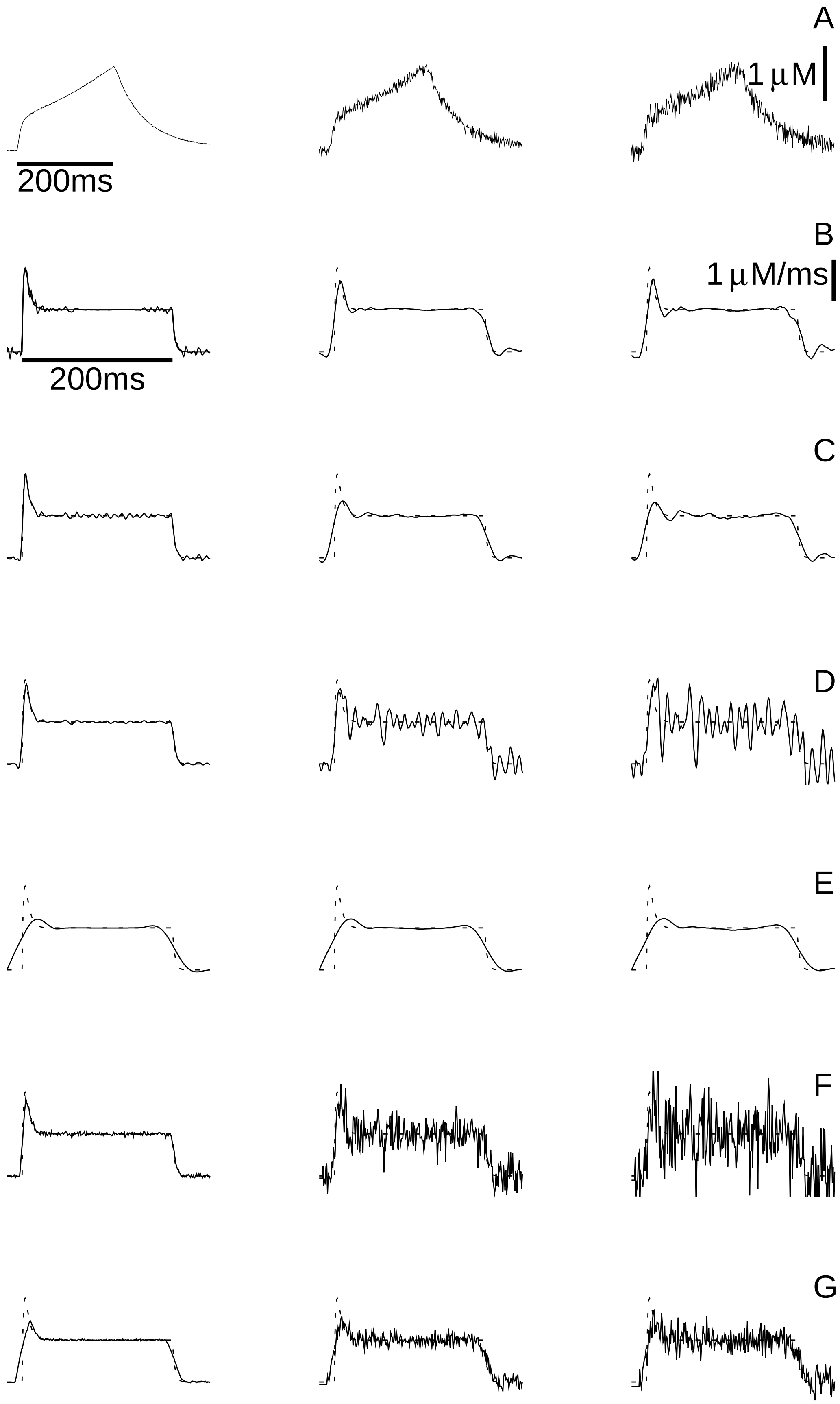

Figure 7:

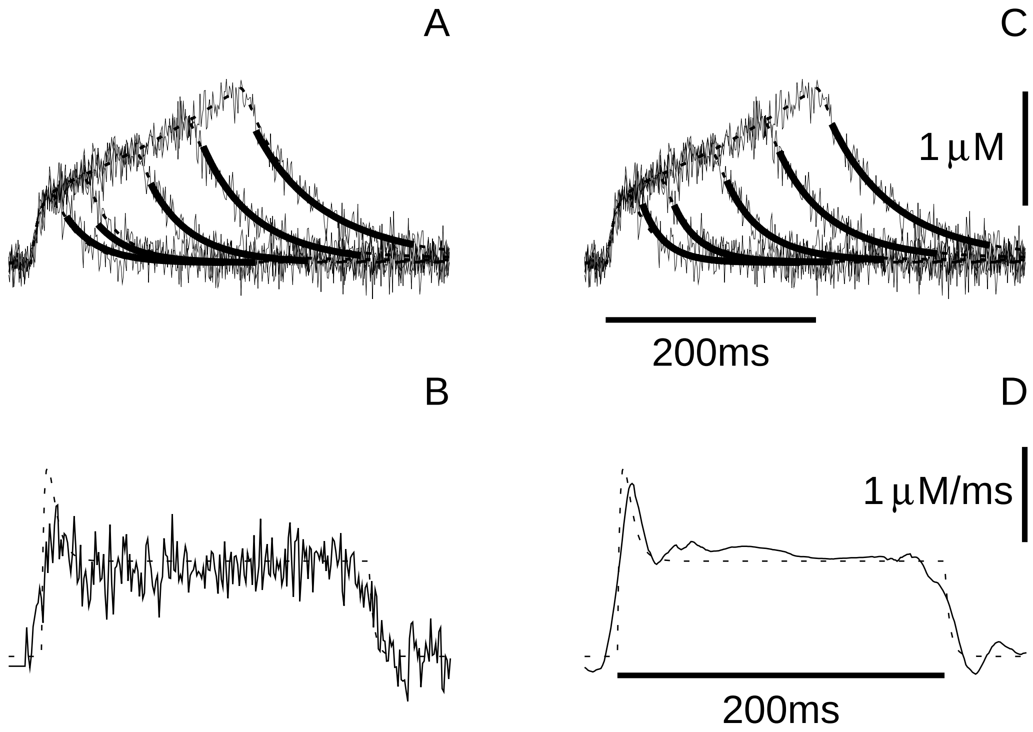

Figure 8:

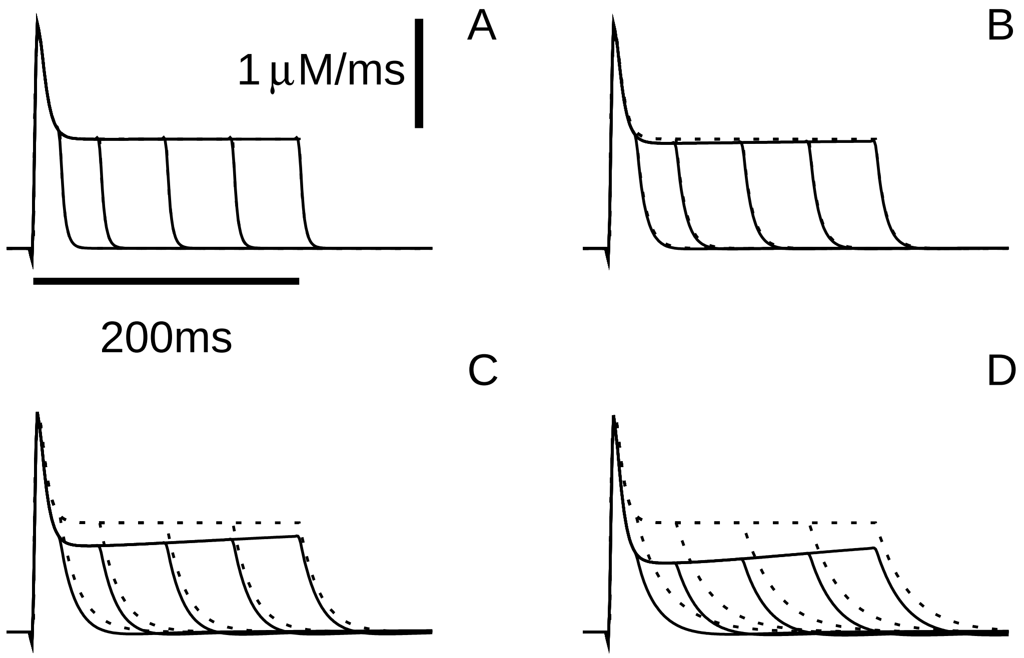

Figure 9:

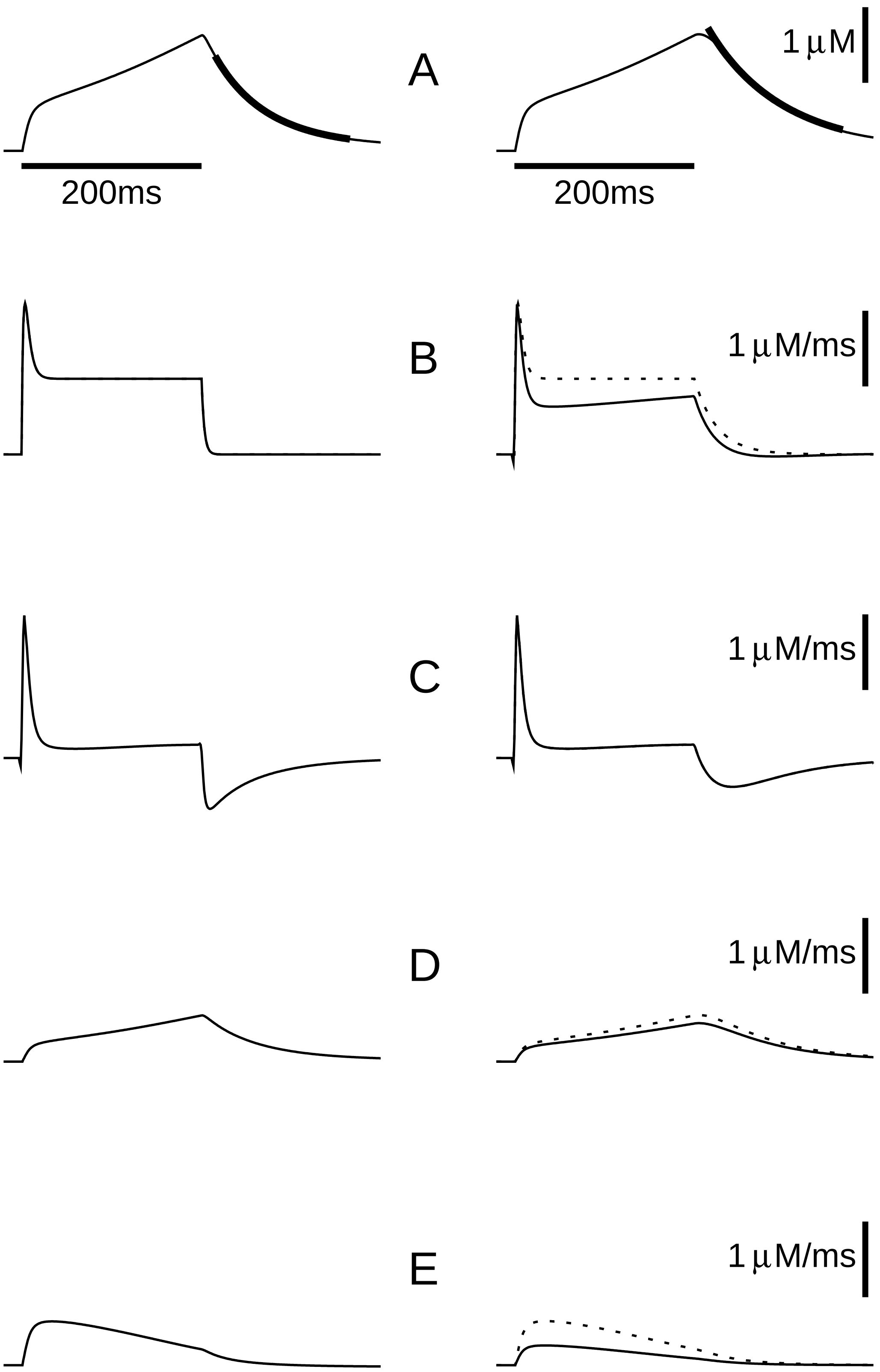

Figure 10:

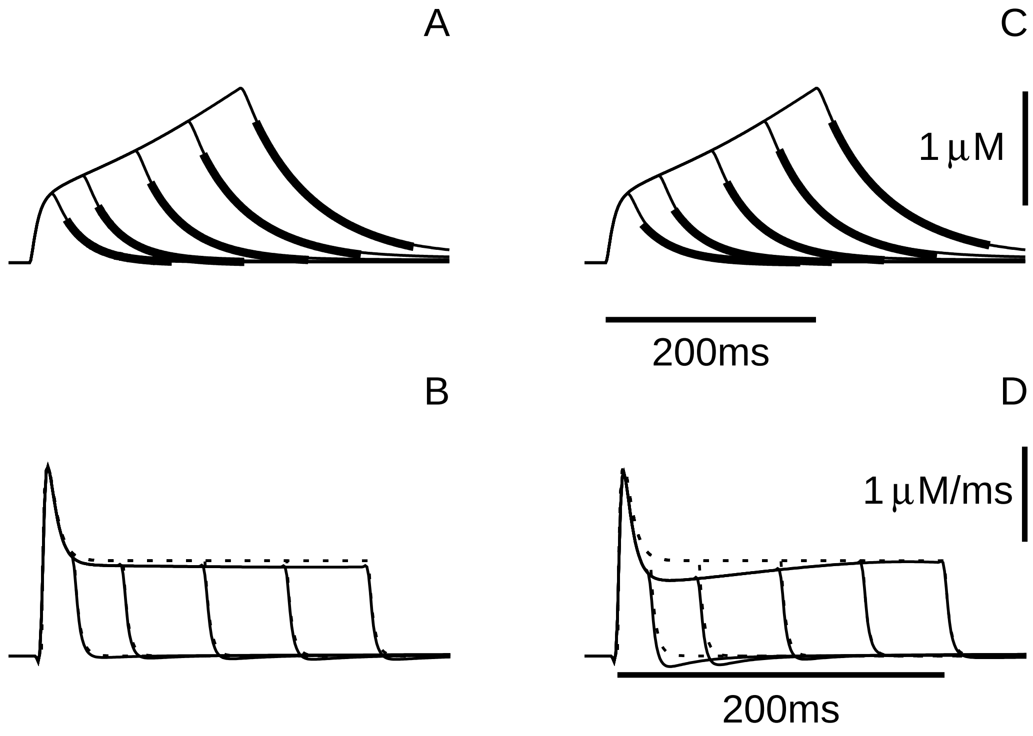

Figure 11:

Table 1:

starting parameters	no constraints FIX	FREE	positivity constr. FIX	FREE	method
	2	2	2	2	IV
10, 0.3, 100, 400	5	5	5	5	MS3
	5	5	5	5	MS5
	3	3	7	7	IV
20, 0.6, 200, 800	6	6	9	8	MS3
	6	6	8	8	MS5
	3	3	8	13	IV
5, 0.15, 50, 200	6	6	5	6	MS3
	6	6	5	5	MS5
	D	D	D	D	IV
0.1, 0.1, 100, 100	D	D	8	13	MS3
	D	D	D	D	MS5
	D	D	12	D	IV
1, 1, 1000, 1000	D	D	8	9	MS3
	D	D	11	11	MS5
	D	D	D	D	IV
1, 1, 100, 100	9	6	8	6	MS3
	9	D	7	7	MS5
	D	D	N	L	IV
1, 1, 10, 10	D	D	10	7	MS3
	D	D	9	9	MS5
	D	D	D	L	IV
1, 1, 1, 1	D	D	D	12	MS3
	D	D	D	11	MS5

Table 2:

A: parameter starting values: 5, 0.15, 50, 200

$\sigma[\mu M]$	IVa	IVb	IVc	MS3	MS5	MS9
0.005	8	D	9	5	5	6
0.01	8	8	8	5	5	7
0.02	8	10	9	5	5	9
0.05	D	9	L	6	6	7
0.1	D	10	8	8	7	10
0.2	D	D	12	41	11	15

B: parameter starting values: 20, 0.6, 200, 800

$\sigma[\mu M]$	IVa	IVb	IVc	MS3	MS5	MS9
0.005	7	8	7	10	9	7
0.01	8	8	7	10	9	7
0.02	9	9	7	10	9	8
0.05	D	D	8	22	8	8
0.1	D	D	N	9	7	7
0.2	D	D	L	8	7	8